The International Journal of Advanced Manufacturing Technology (2023) 127:3135–3156
https://doi.org/10.1007/s00170-023-11709-2

CRITICAL REVIEW

Recent research progress of foam metals welding: a review

Mengnan Feng[1,2] · Liang Ren[1,2] · Ziyao Wang[1,2] · Dequan Meng[1,2] · Shuo Wang[1,2] · Peng Wang[1,2]

Received: 26 October 2022 / Accepted: 4 June 2023 / Published online: 16 June 2023

Abstract
The unique porous structure of foam metal imparts a variety of advantageous properties, including low weight, reduced density, extensive specific surface area, efficient sound and energy absorption, exceptional thermal insulation, effective electromagnetic shielding, and outstanding electrochemical behavior. As a result, foam metals are deemed crucial for both functionalizing structural materials and structuring functional materials, finding widespread application in electronics, chemicals, machinery, and aerospace sectors. Currently, the welding of foam metals is a subject of significant interest and ongoing research, with numerous studies aimed at refining the welding process. This review provides an overview of the current state-of-the-art research on foam metal welding and evaluates the feasibility of different welding techniques from a methodological perspective. A comparison of the efficiency and efficacy of various welding approaches in the preparation of foam metal joints is performed to highlight their strengths and limitations. Finally, this paper summarizes the current developments in foam metal welding and provides insights into the future trajectory of this field.

Keywords Foam metal · Fusion welding · Pressure welding · Brazing

1 Introduction

Porous foam metal can be conceptualized as a novel composite material that embodies a coexistence of inhomogeneous metal skeleton and air phase, and can be characterized as a solid matrix with internal pores. The numerous interfaces between the pores and the metal matrix bolster the interaction of defects between the two phases, such as dislocation motion and plastic slip in the flawed region, leading to a substantial reduction in energy via repeated reflections. Thus, the foam metal displays remarkable damping behavior, sound absorption, energy absorption, buffering capacity, and exceptional compression and fatigue properties, attributed to its unique structural composition [1–4].

✉ Mengnan Feng
fengmn@stdu.edu.cn

✉ Peng Wang
wangpengcl@tju.edu.cn

[1] Hebei Key Laboratory of Advanced Materials for Transportation Engineering and Environment, Shijiazhuang TieDao University, Shijiazhuang 050043, China

[2] School of Material Science and Engineering, Shijiazhuang TieDao University, Shijiazhuang 050043, China

In terms of electrochemical properties, the interchangeable metal skeleton structure induces eddy currents and an alternating magnetic field upon connection to an AC current, thereby imparting reliable electromagnetic shielding. Furthermore, the presence of a thin oxide layer on the surface of the skeleton of the foam metal results in exceptional thermal conductivity, which positions it between metallic materials and thermal insulation materials. In conclusion, foam metal exhibits a multitude of advantageous properties such as low weight, high specific strength, sound absorption, high energy absorption, electromagnetic shielding, heat insulation, reduced density, extensive specific surface area, and exceptional electrochemical behavior, among others, owing to the integration of the excellent characteristics of metal and foam metal [5–7]. This has enabled the multifunctionalization of structural materials and the structuring of functional materials [8, 9]. With its main characteristics shown in Fig. 1, foam metal finds wide application in the electronics, chemical, mechanical, and aerospace fields [10, 11]. Advanced industrial nations such as the USA, Britain, Germany, Japan, and Russia have placed foam metal at the forefront of new material research in the twenty-first century [1–11].

At present, the exploration of foam metal remains in its nascent stage, garnering substantial attention from

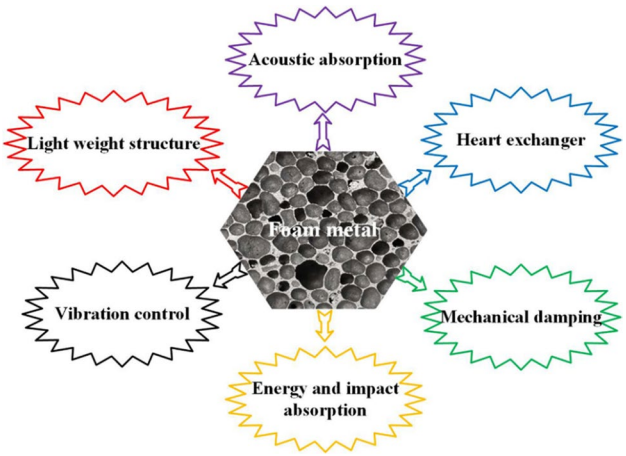

Fig. 1 The main characteristics of foam metal

researchers and eliciting extensive inquiry into its processing and preparation methods, mechanical properties, microstructure, and electrochemical characteristics [12, 13]. Despite the abundance of research findings, a more integrated and sophisticated understanding of foam metal is necessary to further advance the field. In recent years, the unique attributes of foam metal have garnered increasing recognition from the industrial sector, leading to the gradual implementation of foam metal in industrial production.

To cater to varying production processes and application needs, foam metal materials of diverse morphology and porosity can be synthesized. For instance, closed-pore foam metal produced through the foaming method (as depicted in Fig. 2a) and some open-cell foam metal with low porosity tend to be utilized as structural materials, while open-cell foam metal boasting three-dimensional skeleton structures produced via the electrodeposition method, as illustrated in Fig. 2b, and possessing porosities of 96% or higher have gained widespread attention for their use as high-capacity battery collectors, electrochemical reaction electrodes, or catalyst carriers [15–19]. This trend is also evident in the fields of chemical cells and fuel cells, where the application of foam metal is becoming increasingly prevalent [15–22].

Welding technology, as a pivotal aspect of secondary processing, is critical in facilitating the increased application of foam metal in various industrial settings. Since the mid-twentieth century, there has been a worldwide competition in the research and development of welding methods specifically designed for the joining of porous foam metal. Currently, the focus of academic research is primarily directed towards low-porosity open-cell foam metal used as structural materials and the welding of foam metal in closed-cell configurations. The porous structure of foam metal, with its highly randomized distribution and tendency to collapse, presents unique heat exchange properties, including exceptional heat resistance and the ability to maintain structural integrity at temperatures exceeding its melting point. Furthermore, its large specific surface area and propensity for forming complex three-dimensional flow patterns result in remarkable heat dissipation capabilities. However, conventional welding methods often prove challenging in effectively welding foam metal.

Welding technology is a crucial advancement in the process of joining high-porosity open-cell foam metal, which possesses an overall structural integrity and physical continuity, and is relatively easy to implement. Despite the homogeneous microstructure of open-cell foam metal, their propensity for fracture during periods of deformation, along with their lower tensile and compressive properties compared to closed-cell foam metal, makes welding such materials a challenging endeavor [19]. The three-dimensional skeleton-like structure of high-porosity open-cell foam metal has yet to be widely studied [23–29]. However, attempts have been made to utilize ultrasonic welding technology to maximize the preservation of the structure and properties of open-cell foam metal while achieving high welding efficiency, short welding time, low heat input, and precision control [30, 31]. Despite these efforts, the exploration and development of efficient and stable open-cell foam metal welding processes and mechanisms are ongoing. Traditional and emerging joining techniques for foam metal, such as glue joints [32], laser beam welding [33–37], resistance spot welding [38], brazing [39], diffusion welding [40], friction stir welding (FSW) [41], and ultrasonic

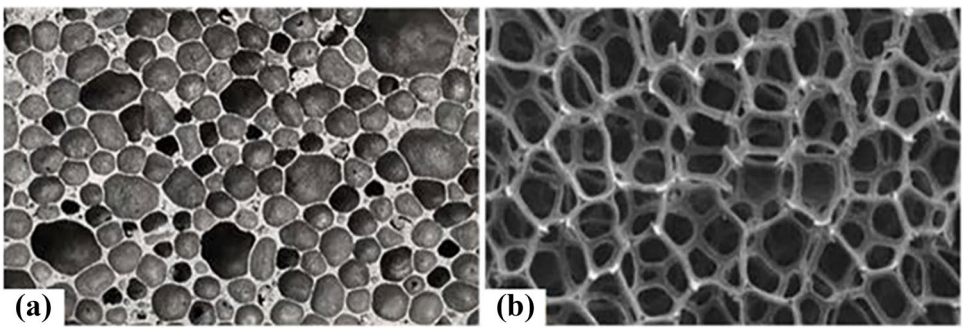

Fig. 2 The classification of foam metal: (**a**) closed-cell structure, (**b**) open-cell structure [14]

Table 1 The summary of the previously studies for foam metal welding

Welding method	Welding material	Welding form	Welding properties	Application
Laser welding	Cu60Zn40(wt%) solid plates (1 mm)/foam plate (about 10 mm) [33, 34]	Lap welding	The joint strength was 83 MPa (50% of the plate/block joint strength)	Not given (early exploration)
Laser welding	Foam (13 mm)/AlSi10 plate (2 mm) [37]	Foam/plate/foam	The foam structure was somewhat densified	Construction
Laser welding	Foam plate /foam plate(13 mm) [45]	Foam/foam	The tensile strength was 0.4 MPa	Not given (early exploration)
Laser welding	Foam plate/AlSi10 plate (1 mm) [45]	Foam/filler/foam	The tensile strength was 2.5 MPa (similar to the base material)	Not given (early exploration)
Melt inert gas welding	4047/5356 Al alloy/closed-cell Al foam (10 mm) [46]	Lap welding	The bending tensile load was 714.13 N	Sandwich composites
Tungsten inert gas welding	AlSi9 foam/AlSi9 foam and AlSi9 foam/solid Al plate [45]	I-beveled	The tensile strength was 2.6 MPa (close to the base material)	Not given (early exploration)
Friction stir welding	AA6061-T6 Al foam plate (3 mm)/Al plate [47]	Sandwich construction	The bending strength was 32.4 MPa	Aerospace, shipbuilding , automotive
Friction stir welding	ADC12 Al alloy plates/foaming agent (3 mm) [48]	Sandwich construction	The fracture occurred in the foam metal	Components of automobiles
Ultrasonic welding	1A99 Al plate (0.3mm)/open-cell Cu foam (0.2mm) [30]	Lap welding	The tensile load was 89.15% of the base material	Thin-film electrode
Ultrasonic welding	Ni foam sheet (0.2 mm)/pure Al sheet (0.3 mm) [31]	Lap welding	The tensile load was 58.0% of the base material	Current collector, catalyst support
Brazing	Ti-6Al-4V layer (0.8 mm)/Ni foam (0.9 mm) [39]	Butt welding	The yield strength and shear strength were 1.27 MPa and 1.44 MPa	Buffer layer

welding [30, 31, 42–44], have been studied and the relevant results are summarized in Table 1. However, these techniques are still limited by factors such as the difficulty of accurately controlling the welding energy, stringent requirements for the welding environment, unavoidable collapse and densification of the pore structure, unsatisfactory joint strength, and a lack of practicality.

This paper aims to investigate various welding approaches for foam metal in various application scenarios and to comprehensively survey the current state and advancements in the fabrication of foam metal and the welding of foam metal/sheet metal (FM/SM) through fusion welding, pressure welding, and brazing methods. Additionally, it endeavors to offer an outlook on the future prospects of foam metal welding research.

2 Fusion welding of foam metal

The extensive application of foam metal, owing to its remarkable properties, has inspired a multitude of researchers worldwide to experiment with various welding processes to effectively join foam metal. The fusion welding method, in particular, has garnered considerable attention, as it requires the material to be brought to a melting point, which results in a robust joint with ample load-bearing capabilities. However, this method also results in significant damage to the foam structure, making it more appropriate for the connection of foam metal's structural components. The development of an optimal fusion welding process hinges upon the precise and focused control of heat input, which necessitates avoiding excessive damage to the foam structure. Selecting a suitable welding method, therefore, is critical. Currently, the most commonly used fusion welding methods for joining foam metal in academia include laser welding and arc welding.

2.1 Arc welding of foam metal/sheet metal or foam metal/foam metal

Arc welding, as a process that converts electrical energy into the thermal and mechanical energy indispensable for welding and subsequently the joining of metals, has garnered widespread recognition and usage. This owes to its attributes of being lightweight, flexible, and its ability to effectively weld a broad spectrum of metal materials, ranging in thickness and structural shape. As a result, arc welding has become the most ubiquitous welding method in contemporary industrial production.

The application of melt inert gas (MIG) welding presents the advantage of compact apparatus size, ease of installation, and low cost of equipment, making it a suitable option for welding thicker plates with thicknesses of up to 1.6 mm, including materials such as stainless steel, Al, and Al alloys. The feasibility of using MIG welding for the preparation of FM/SM joints of a particular thickness is evident. However, the introduction of shielding gas and residual foaming agent TiH_2 hydrogen in the high-temperature welding environment can result in a significant number of spherical voids in the weld fusion zone, potentially reducing the reliability of the joint. In a study by Shih et al. [49], in 2011, MIG welding was attempted on 4047 and 5356 Al alloy with thin closed-cell Al foam by using a plate as a welding filler material placed above the Al foam. The use of pure argon as the shielding gas during the welding process resulted in a weld cross-section with numerous spherical bubbles observed in the weld, composed of elements such as Al, O, and Mg, as shown in Fig. 3. The longitudinal bending tensile strength of the MIG-welded closed-cell Al foam/Al sheet joints was found to be 72.87 kgf, with fracture occurring on the Al foam side rather than in the weld fusion zone, indicating the superior strength of the MIG-welded joint in comparison to the parent material, even in the presence of porosity at the weld joint.

The tungsten inert gas (TIG) welding technique is widely utilized for welding an array of non-ferrous materials such as Al alloys, Mg alloys, Ti alloys, stainless steel,

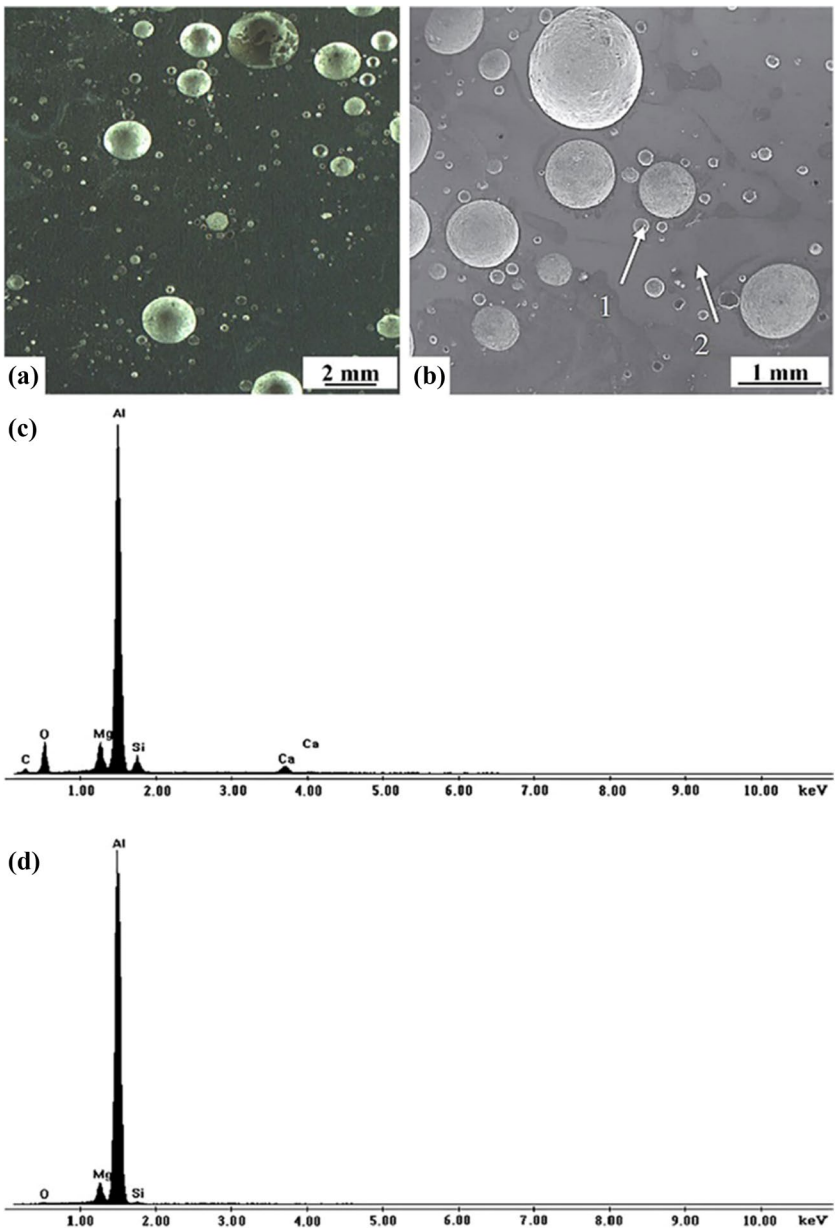

Fig. 3 The results analysis of SEM images and EDX of weld pore in arc welding of Al foam: (**a**, **b**) pores in the fusion zone, (**c**, **d**) the composition of the position 1 or 2 shown in Fig. 3b [49]

high-temperature alloys, and refractory reactive metals among others [50]. This is due to its notable attributes, including effective air isolation, a stable arc, and easily adjustable heat input. In a study by Nowacki et al. [45], TIG welding was used to prepare joints of AlSi9 foam and AlSi9 foam/solid Al sheet. The single-pass TIG welding was performed using a 1.6-mm diameter AlSi5 welding wire as filler material and argon gas of 99.996% purity as a shielding gas, with a current range of 15–30 Amperes in AC mode. The macroscopic morphology of the three types of welded joints prepared is presented in Fig. 4. Densification of extensive regions of the foam metal was observed in all cases. However, welding the foam metal using low-current TIG alone could not prevent the collapse of its structure, resulting in unavoidable joint defects. To enhance the efficiency and reliability of the fusion-welded foam metal joint connection, an arc heating and pressing process was performed prior to welding, albeit it caused some degree of damage to the foam structure.

The work of Nowacki et al. [45] was informed by the prior research of Haferkamp [37]. Despite the inherent limitations of their complex experimental design, it has undoubtedly expanded the scope of the study of foam metal welding.

The feasibility of conventional arc welding techniques for foam metal welding relies on the refinement of the welding process to minimize the adverse effects of welding defects such as porosity, inadequate penetration, and increased stress concentrations due to the densification of the foam structure.

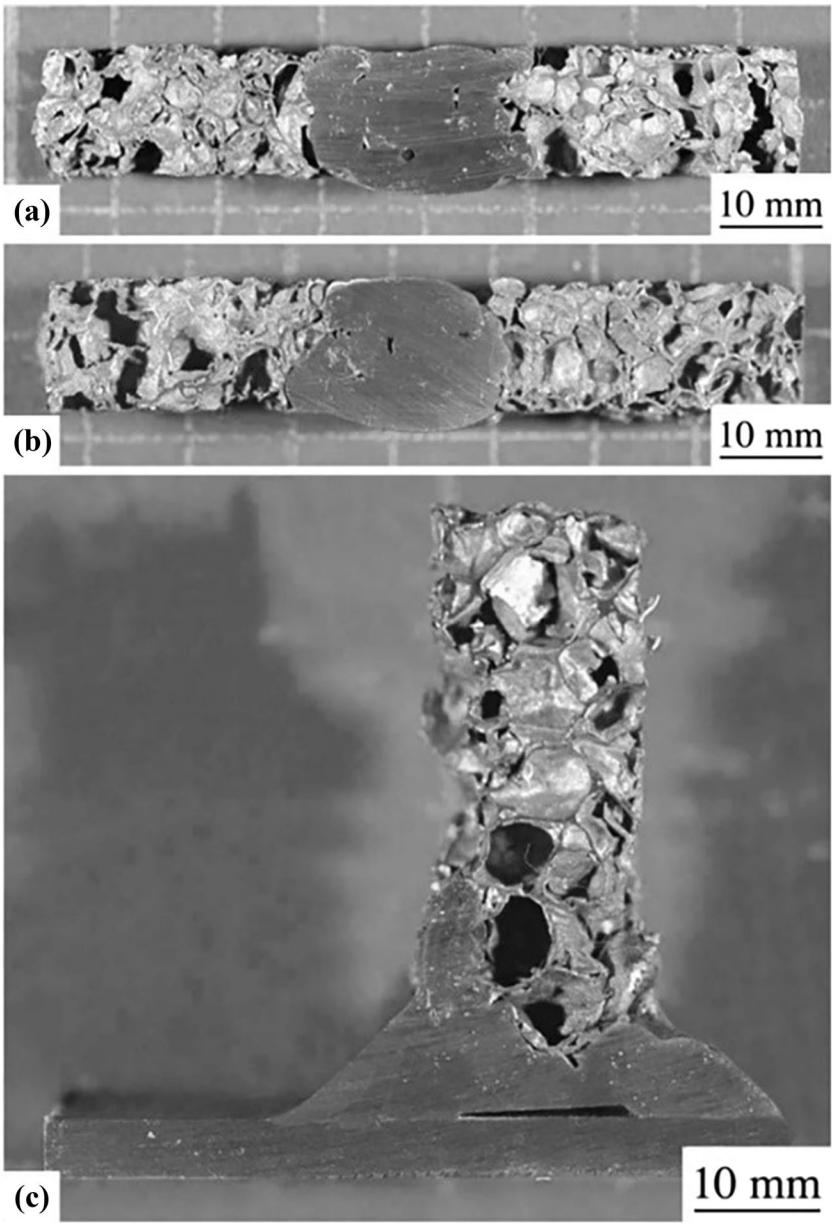

Fig. 4 The macroscopic morphology of three different forms of TIG welding: (**a**) Y-beveled sample, (**b**) I-beveled sample, and c T-joint sample [45]

Additionally, the choice of arc welding process must also account for the softening of the heat-affected zone (HAZ), as the fractures of joints produced through arc welding typically occur in this region. In terms of practical applications, the primary requirement of joints produced through welding foam metal using arc welding is load-bearing capacity, with the aim of reducing foam density in the joint to decrease stress concentrations and increase the joint's load-bearing capacity.

2.2 Laser welding of foam metal/sheet metal or foam metal/foam metal

The application of laser welding as a cost-effective, flexible, and precisely controllable high-energy beam welding technique presents numerous benefits over traditional methods. The methodology enables a precise control over the minimum required heat input to shape and process the desired foam metal and joint. Additionally, as laser welding is a non-contact welding process, it eliminates any potential mechanical loss to the foam base metal. Furthermore, the laser can be guided by optical instrumentation to concentrate the welding energy in areas of specific interest, making it an ideal choice for three-dimensional hole structures in foam metal or welding environments with obstacles.

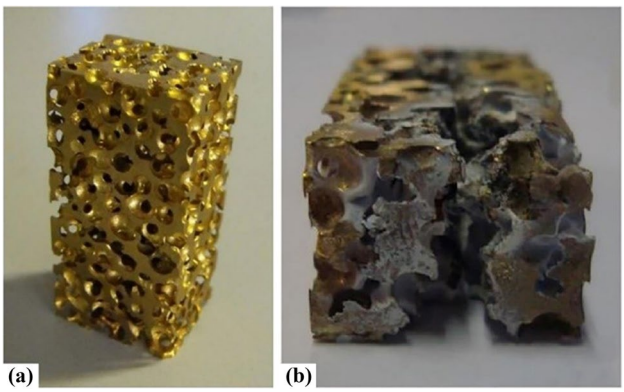

Fig. 5 The macroscopic morphology of Cu60Zn40 foam: (**a**) pre-welding, (**b**) post-welding [33]

The localized and precise control of energy, provided by laser welding, is of utmost significance for the welding and three-dimensional printing of foam metal.

In 2014, Biffi et al. [33] attempted to weld an open-cell Cu60Zn40 (wt.%) foam metal using a 1 kW continuous-wave fiber laser. The open-cell foam metal was prepared through liquid-phase immersion with a porosity of 65–70% as depicted in Fig. 5a. Experimental examination of laser overlay welding on the foam metal plate revealed that the absence of proper filler material resulted in unreliable joint formation, as the laser spot aperture was smaller than the porous structure of the foam metal and the random pore configuration of the foam metal resulted in a reduced contact rate at the welding interface, resulting in burning through of the foam metal as shown in Fig. 5b.

In order to establish a secure interaction between the laser and the foam metal, an attempt was made to fabricate a laser lap joint between a Cu60Zn40 foam metal and a 1-mm-thick cold-rolled sheet. The joint was created by positioning the cold-rolled sheet on top of the foam metal, as depicted in Fig. 6a. To mitigate the evaporation of low-melting and boiling point Zn elements during the welding process, a multi-nozzle system, as depicted in Fig. 6b, was employed to ensure adequate coverage of argon gas flow.

The cross-sectional metallographic organization of the lap joint, as depicted in Fig. 7, reveals that under the welding conditions with speeds ranging from 5 to 20 mm/s, a portion of the melted sheet material is incorporated into the foam hole structure, compensating for the lack of interface contact and leading to a more comprehensive weld. Notably, no cracks were observed in the weld or the HAZ. The findings of this study demonstrate that a dependable connection between the sheet and foam metal can be established through laser welding under specific pre-determined conditions. However, it is worth noting that despite the resolution of the issue of weld formation resulting from the randomness of foam metal/plate surface contact through the inflow of molten metal from the solid plate, the joining behavior of the plate and foam can only occur at locations where the hole structure serves as a boundary. As a result, the distribution of weld penetration in the foam metal is inconsistent,

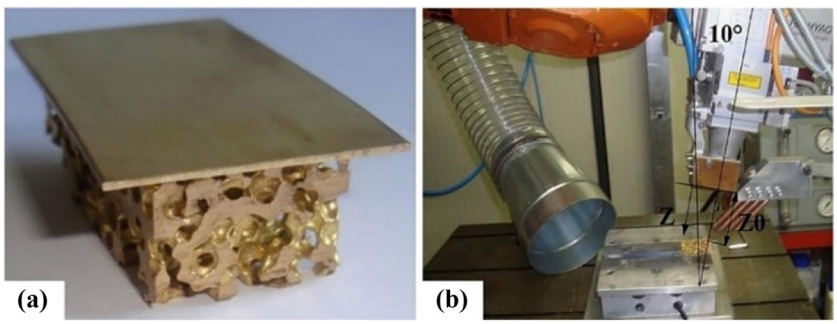

Fig. 6 The physical view of laser welding of Cu60Zn40 foam: (**a**) lap structure of sheet and foam metal, (**b**) system of shielding gas [33]

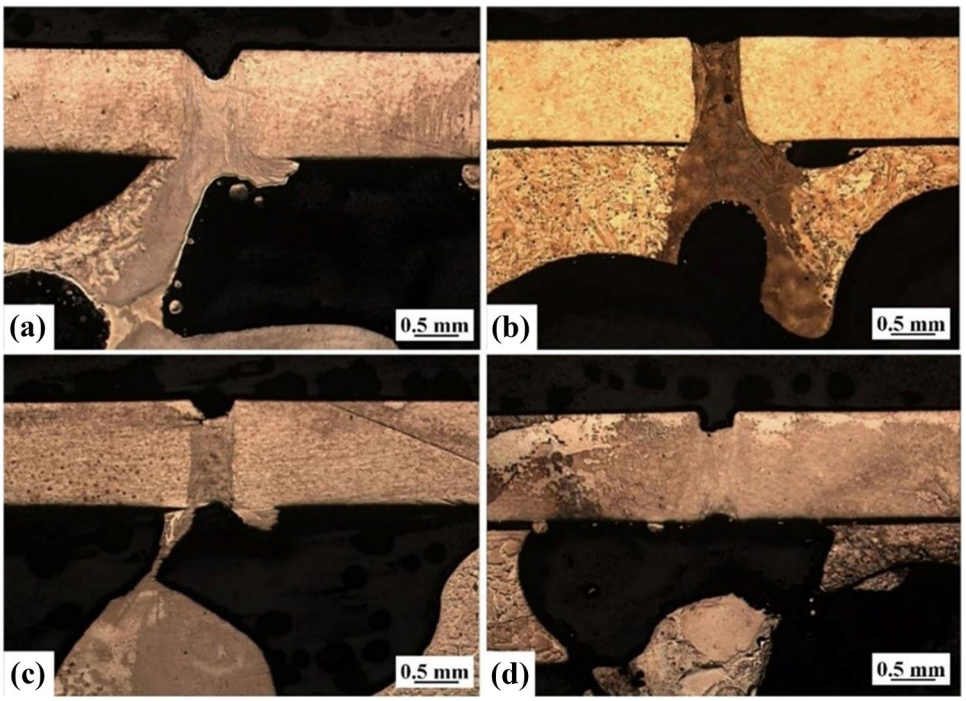

Fig. 7 The microstructure of the weld seam at different welding speeds in laser welding of Cu60Zn40 foam: (**a**) 5 mm/s, (**b**) 10 mm/s, (**c**) 15 mm/s, and (**d**) 20 mm/s [33]

thereby reducing the efficiency of foam metal connection during laser welding.

In 2016, Biffi et al. expanded their investigation into the mechanical properties and microstructural characteristics of Cu60Zn40 FM/SM laser–welded lap joints [34]. The microstructural evolution across the various regions of the sheet and foam joints is depicted in Fig. 8. The sheet joints and foam joints exhibit a clear manifestation of the molten region in their fine dendritic organization, as depicted in Fig. 8a and c, which may be attributed to the rapid condensation process inherent to laser welding. However, the HAZ of the foam joint comprises both fine and coarse dendrites, with the former potentially arising from the high cooling rate of the laser process, and the latter resulting from the low cooling rate of the casting process. This disparity in the morphology of the HAZ between the foam joint and the sheet joint is a significant finding.

The rapid condensation process of laser welding is found to have resulted in the attainment of the highest levels of microhardness in both the sheet and foam metal, with values of 125 HV and 135 HV, respectively, at the center of the weld, as depicted in Fig. 9a. The post-heat treatment of the Cu alloy, however, has produced a marked reduction in the hardness of the HAZ of the sheet, with an estimated value of approximately 85 HV. In contrast, the softening effect in the HAZ of the foam joint appears to be less pronounced, potentially due to the scattering of microhardness values and the bimodal dendrite structure of the foam. As depicted in Fig. 9b, the shear tensile strength of the plate/foam metal

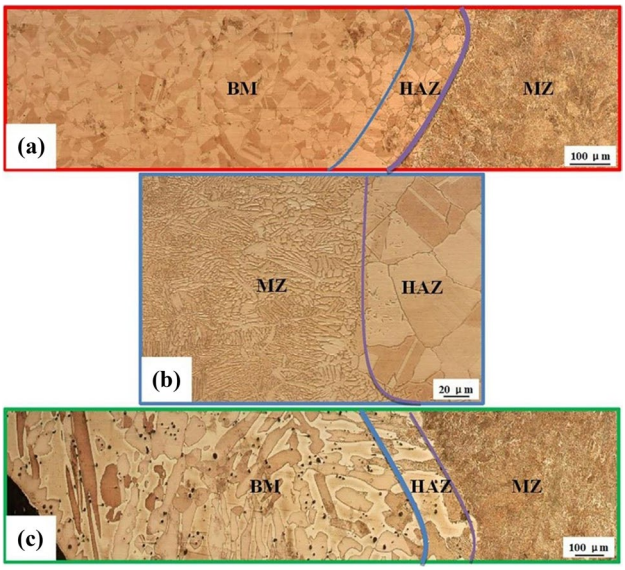

Fig. 8 The microstructural evolution at the FM/SM laser–welded joint: (**a**) transition from melt zone (MZ) to base metal (BM), (**b**) transition from MZ to HAZ in filled plates, and (**c**) transition from MZ to HAZ and then to BM in foam metal [34]

laser lap joint was determined to be 83 MPa, which constitutes roughly 50% of the strength of the plate/block joint. This reduction in strength is attributed to the presence of pores within the foam structure, and the stress fluctuations observed during testing may be due to the irregularity of the weld seam and the foam metal's energy absorption properties.

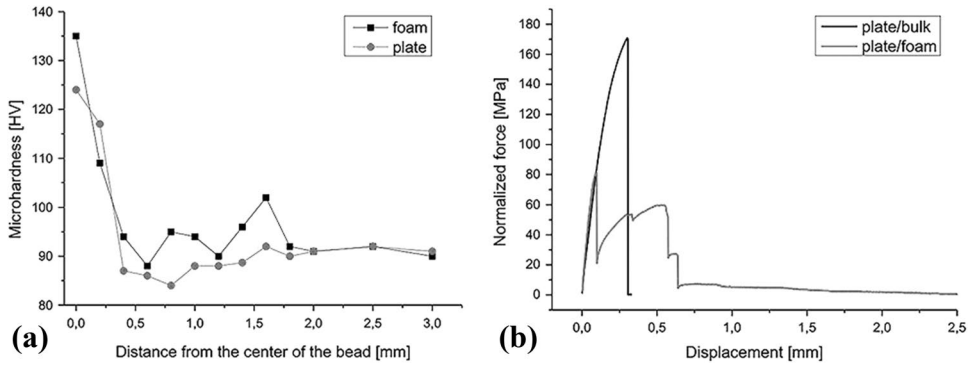

Fig. 9 The mechanical properties of the laser-welded Cu foam metal joints: (**a**) microhardness profile, (**b**) shear stress/strain curve [34]

Table 2 The forms and fillers for laser welding of foam metals [45]

Specimen number	Filler form and material
1	Filler wire of Al
2	Filler in the form of AlMgSi1 with 1 mm thickness
3	Filler in the form of non-porous precursor with powder compact AlSi10 plate of 2 mm thickness and foaming agent-TiH_2

The lion's share of studies on foam metal laser welding has been devoted to exploring the welding of foam metal with solid plates, with the latter being predominantly utilized as filler material, and relying on a plate-on-top-of-foam lap welding pattern to attain trustworthy laser-welded joints. Haferkamp et al. [37] were pioneers in this domain, having developed a laser welding process for AlSi10 closed-cell foam metal and devised three distinct welding patterns, as outlined in Table 2, with two of these design forms depicted in Fig. 10. The closed-cell foam used boasts a density of 0.5 g/cm^3, and is comprised of AlSi10 alloy manufactured via powder metallurgy. A CO_2 laser with a power output of 6 kW was utilized, with helium serving as the shielding gas during the welding process.

When it comes to employing wire as filler material for foam metal welding, as illustrated in Fig. 10a, a wire feed speed of less than 5 m/min at a welding speed of 1 m/min results in a recessed weld surface. However, a more favorable joint can be obtained by increasing the wire feed speed to 8 m/min. Deep penetration was accomplished by interposing the filler in the form of a non-porous Al sheet between the joined foam metals (Fig. 10b), with a laser beam welding speed of 1.9 m/min. While the quality of the resulting joint is commendable, the presence of a substantial amount of filler material in the foam pore structure results in some degree of densification of the foam structure. By using a non-porous foam precursor made of AlSi10 powder and TiH_2 blowing agent, Al foam was welded to the joint surface of the foam metal, resulting in a joint structure akin to that of the Al foam parent material. Nevertheless, the phenomenon of foam structure densification still persists.

The study conducted by Nowacki et al. [45] incorporated seven distinct experimental conditions as documented in Table 3, with the macroscopic morphologies

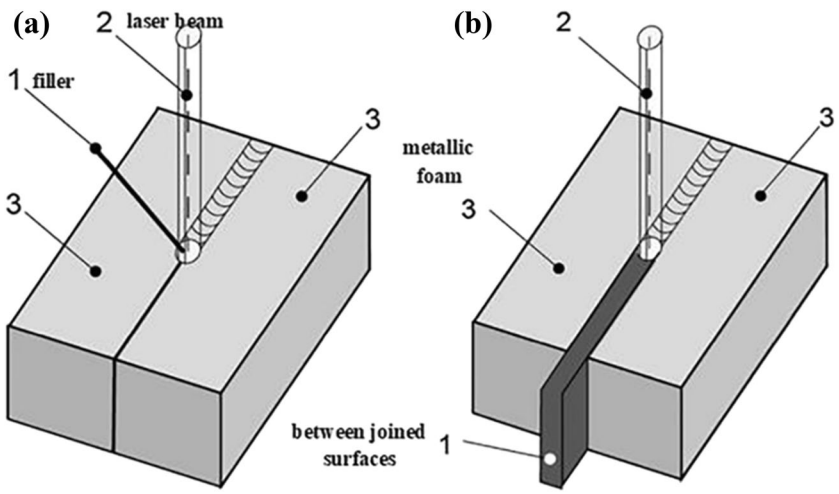

Fig. 10 The two different forms of the filler material in the laser welding of foam metal: (**a**) filler wire [46], (**b**) filler sheet [37]

Table 3 The configuration of laser welding tests of foam metal [45]

Specimen number	Laser type or welding form	Laser diameter (μm) or focus dimension (mm×mm)	Laser power	Welding speed or exposure time
1	Trumpf TruDisk 3302 disk laser	200 μm	800 W	1 m/min
2	Trumpf TruDisk 3302 disk laser	200 μm	400 W	1 m/min
3	HPDL Rofin Sinar DL 020 diode laser	1.8 mm×6.8 mm	800 W	0.1 m/min
4	Butt welding of I-beveled specimens without filler under Trumpf Trudisk 3302 disk laser	200 μm	400 W	1 m/min
5	HPDL Rofin Sinar DL 020 diode laser with the 1.6 mm wire $AlSi_5$ as filler metal	1.8 mm×6.8 mm	800 W	0.1 m/min
6	Spot welding, butt joint, and I-beveled under Rofin Performance laser	200 μm	800 W	3.0 ms
7	Spot welding, butt joint, and I-beveled under Rofin Performance laser	200 μm	2000 W	3.6 ms

of the foam metal joints represented in Fig. 11. The macroscopic morphologies of the specimens 1–3 in Table 3 displayed a range of foam structure collapse degradation, as depicted in Fig. 11a–h. In these instances, the foam structure densification was substantial enough to form a more coherent weld, yet the area of the weld was expansive and deviated significantly from the surrounding base material structure, leading to an increased stress concentration. When the disk laser power was 800W, the length of the bridge connection at the joint was diminished and the laser beam may have produced a cutting effect rather than welding the foam metal, as indicated in Fig. 11a. However, when the disk laser power was optimized to a power density of 400W, a substantial connection bridge was established at the joint, as demonstrated in Fig. 11b.

A limited number of interconnections are visible in Fig. 11g, and their irregularity and actual quantity can be further analyzed via Fig. 11h. Figure 11e illustrates that the broad focus of the laser results in substantial collapse of the foam structure and concavity in the welds, and this degradation is challenging to counteract through the use of filler material. In Fig. 11f, it is evident that the joints produced without pre-treatment exhibit limited effective bonds, a result of the difficulty in achieving adequate contact between the foam metal and the laser beam at the intended point of contact. Subsequently, the average static tensile strength of such joints is found to be low across all tests, with fracture occurring at the joints. In contrast, the joint depicted in Fig. 11d guarantees full contact between the foam metal surfaces following pre-weld treatment, resulting in a static tensile strength of the joint as 2.5Mpa, which is approximately equivalent to that of the base material, with fracture occurring in the base material region.

According to preliminary experimental findings, any direct welding of foam metal through fusion welding techniques is likely to significantly impair the joint effectiveness due to the high porosity of the foam metal. In light of this, Nowacki et al. [45] performed two pre-welding processes, arc heating of the Al foam base material and pressing. The arc heating of the base material permits high-temperature plastic deformation of the surface of the base material, thereby enhancing the efficiency of the joint, while the application of pre-weld pressing reduces the porosity of the contact surface and increases the reliability of the joint.

In conclusion, the application of a tailored test methodology and a suitable joint configuration with the plate serving as a filler, laser welding has been demonstrated to effectively achieve a secure bond between the sheet and foam metal with no significant cracks discerned in the weld. The integration of supplementary filamentary or non-porous precursors further enables the joining of foam metal to foam metal, yielding a joint structure comparable to the parent Al foam metal. The concentrated heat input, smaller HAZ, and improved densification of the foam structure imparted by laser welding impart beneficial mechanical properties to the joint, in comparison to arc welding. However, the irregularity of weld formation resulting from the random pore structure of foam metal, combined with the deep melting depth of laser welding, negatively impacts the efficiency and largely limits the mechanical properties of the joint. Additionally, there is still densification of the foam structure in the laser-welded foam metal joints. From a practical standpoint, laser welding presents a viable approach for the fabrication of structural foam joints. Although the foam structures obtained via laser welding are less densified than by arc welding, the joints still fail to meet the functional requirements of foam metal.

Most of the research in fusion welding of foam metal has centered around the optimization of a particular welding method for a specific foam metal, with the aim of obtaining a joint of a certain strength, as fusion welding is predominantly employed for load-bearing applications. The successful preparation of a FM/SM fusion–welded joint heavily depends on the choice of joint form and the development of the welding process.

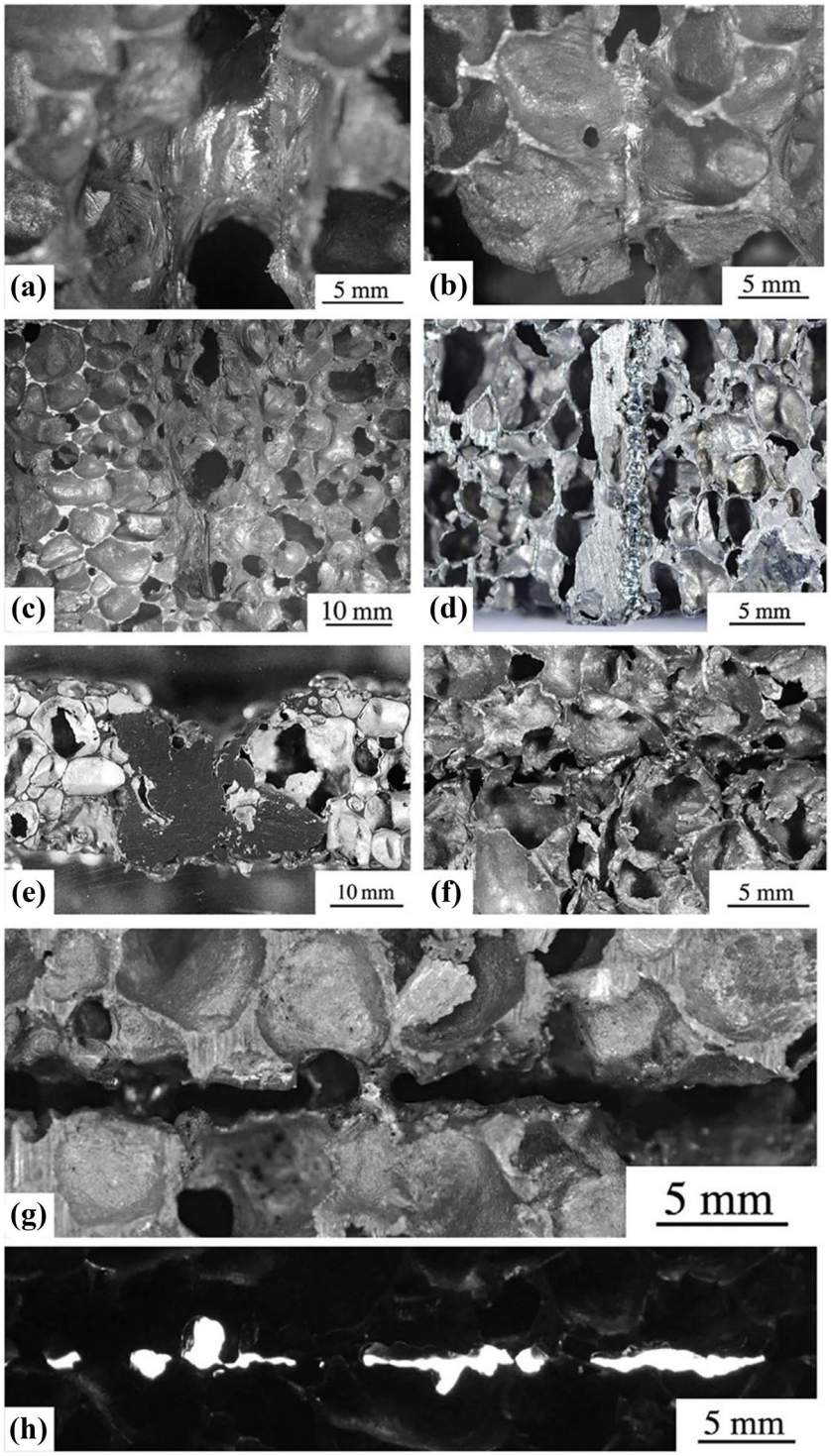

Fig. 11 The macrostructure of representative laser-welded joints of foam metal in Table 3: (**a**) specimen number 1, (**b**) specimen number 2, (**c**) specimen number 3, (**d**) specimen number 7, (**e**) specimen number 5, (**f**) specimen number 6, (**g**) specimen number 4, and (**h**) specimen in contrast light [45]

3 Pressure welding of foam metal

Pressure welding is a method of forging a bond between two metal parts through the application of mechanical pressure, which induces plastic deformation and diffusion of the contacting surfaces, resulting in close and intimate contact. Unlike fusion welding, pressure welding accommodates a broader range of weldable metals, and a portion of the pressure welding methods does not require the melting of metal, rendering it a more suitable method for welding dissimilar metals as documented in various studies [30, 31, 40–43]. In the pursuit of connecting foam metal while avoiding the detrimental effects of collapse and loss of porosity caused by fusion welding, researchers have explored

various pressure welding techniques in an effort to meet the functional requirements of foam metal welds. Significant advancements have been made in this area, catalyzing the progress of research on foam metal welding processes. However, a pressing challenge remains: how to achieve an efficient and reliable connection while preserving the foam metal's unique pore structure to the greatest extent possible.

3.1 Friction stir welding of foam metal/sheet metal

Since its advent towards the close of the previous century, FSW has brought about a revolution in the joining technology of low-melting-point non-ferrous metals, such as Al alloys. Owing to its features of inducing minimal changes to the microstructure of the HAZ, producing low residual stress, and inducing limited deformation of the workpiece, FSW has proven to be highly effective in welding light alloys like Al alloys. In recent years, several scholars have embarked on utilizing FSW for the preparation of foam metal possessing a certain pore structure. Currently, the applications of FSW in the field of foam metal are primarily classified into two categories: first, as a means of precursor foam metal preparation, and second, as a method for welding foam metal.

Hangai et al. [51] devised a novel foaming process aided by the FSW method to form the precursor, which not only overcomes the complicated and costly process, randomness, and difficulty in ensuring uniform distribution of pore structure associated with traditional foaming methods [19, 52, 53], but also enables microstructural modification of metallic materials [54].

Nisa et al. [55] employed FSW for the preparation of 6063 Al foam, as depicted in Fig. 12. A blend of TiH_2 and Al_2O_3 powders was uniformly positioned between the upper and lower 6063 Al plates with dimensions of 150 mm × 100 mm × 3 mm, with TiH_2 serving as the foaming agent and Al_2O_3 acting as the stabilizer. The FSW welding stirrer head moved in the direction illustrated in the figure, resulting in the formation of the precursor, followed by heat treatment, which produced Al foam with 60% porosity after cooling to room temperature. The results of the morphological and compositional analysis of the foamed 6063 Al revealed that FSW facilitated the embedding of the powder mixture into the metal matrix, thus providing the foundation for the formation of the pore structure during heat treatment.

Hangai et al. [56] further expanded upon their previous research regarding the application of FSW in the preparation of foam metal by conducting a study on the point FSW foaming process, as depicted in Fig. 13. The precursor foam was generated through FSW processing of die-cast Al-Si-Cu alloy plates with or without the incorporation of a stabilizer, omitting the use of a foaming agent. The application of

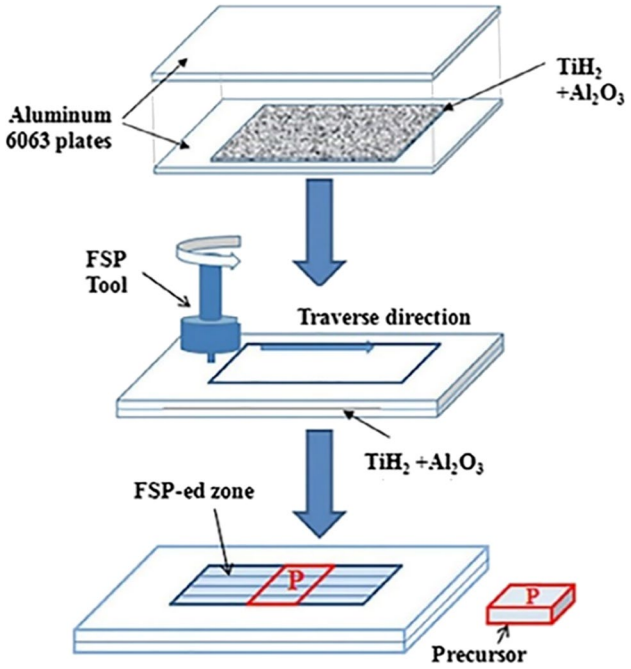

Fig. 12 The diagram of precursor formation to Al foam by FSW [55]

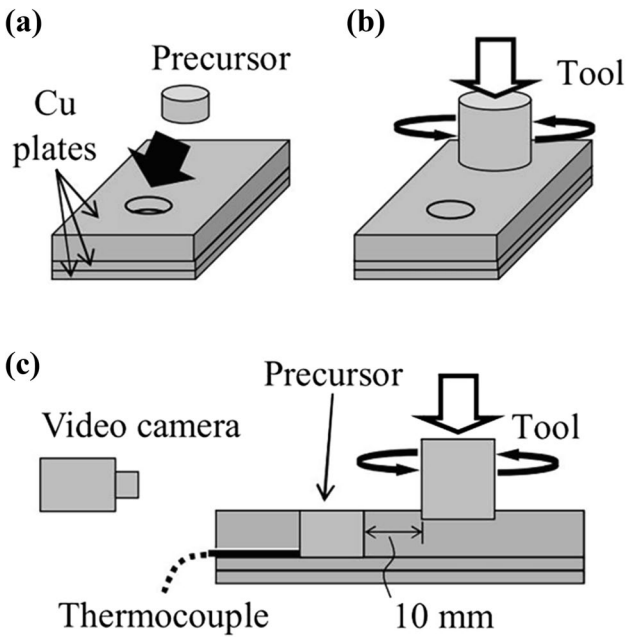

Fig. 13 The schematic diagram of the FSW foaming process of Cu: (**a**) precursor placed in a hole in the Cu plate, (**b**) rotating tool placed on the Cu plate, and (**c**) side view of the foaming process [56]

air-hole foam precursor exclusively enabled the production of Al foam, significantly reducing both energy consumption and cost associated with the preparation of Al foam.

The results of X-ray computed tomography (CT) observations on the prepared Al foam are presented in Fig. 14. The

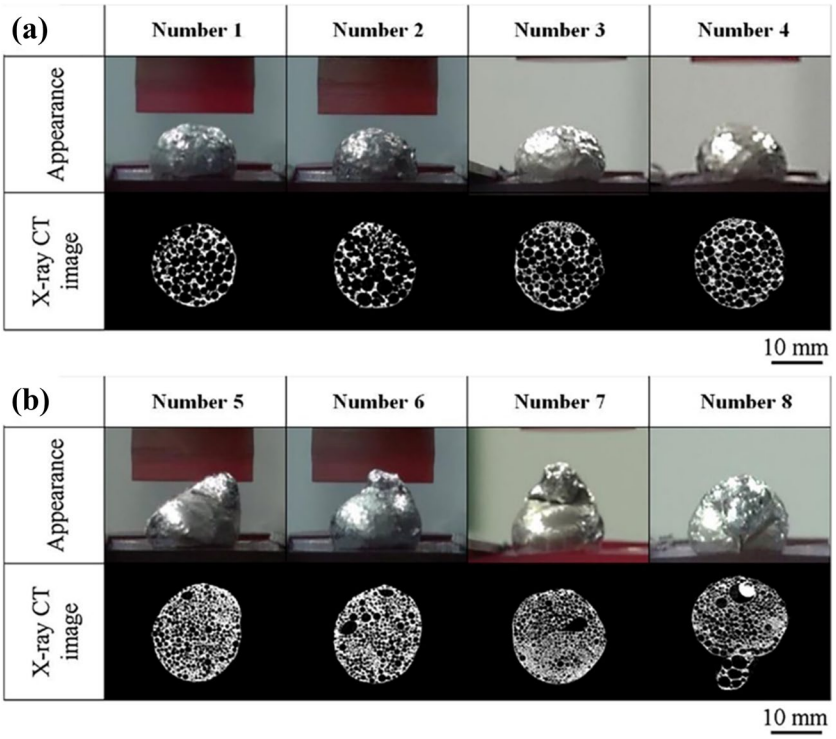

Fig. 14 The cross-sectional CT images of Al foam: (**a**) without Al_2O_3, (**b**) with Al_2O_3[56]

study demonstrates that it is feasible to produce Al foam through friction heat generated during friction stir spot welding without the addition of TiH_2 as a foaming agent. Although Al foam can be obtained without the use of Al_2O_3 stabilizer, incorporating stabilizer during the foaming process leads to a higher expansion rate and finer pore structure, resulting in improved forming and properties of the Al foam.

The application of FSW in the preparation of foam metals is not limited to Al foams, as demonstrated by Sharma et al. [57] who utilized the FSW process to fabricate open-cell Cu foam parts of various shapes and sizes. However, its re-dissolution with the aid of sodium chloride as a spacer material resulted in inadequate uniformity of the formed Cu foam pores. The presence of more uncontrolled factors in this sintering method may affect the performance of Cu foam to some extent.

Building upon the study of utilizing FSW for the production of foam metal, numerous scholars have discovered the possibility of fabricating foam sandwich structures that preserve the low-density and energy-absorbing characteristics of foam metal while significantly augmenting its tensile and flexural strength. Such findings are poised to find application in structural elements [47, 48]. Peng et al. [47] successfully prepared a high-performance Al foam sandwich (AFS) through the application of FSW, and the process flow is depicted in Fig. 15.

The high-performance AFS prepared by FSW exhibited remarkable structural integrity and was devoid of any defects or cracks as depicted in Fig. 16a. Although the stirring head imparted some damage to the foam structure, it was not detrimental to the overall performance of the structure. The cross-sectional scanning electron microscopy (SEM) morphology of the sandwich structure depicted in Fig. 16b demonstrates that the AA6061 Al alloy panel underwent intense plastic deformation, and the flow of metal enhanced the connection between the foam and plate. The results of energy-dispersive X-ray spectroscopy (EDS) compositional analysis displayed in Fig. 16c revealed the absence of intermetallic compounds, which would have otherwise impacted the toughness of the joint. The four-point bending test of AFS revealed that the bending strength of the joints reached approximately 32.4 MPa, indicating its exceptional impact resistance. The specimens displayed an average energy and sound absorption of 0.357 dB and 65.82 dB, respectively, which surpassed the values exhibited by the foam parent material and the Al sheet.

Hangai et al. [48] extended the FSW process for the preparation of precursors to produce die-cast Al alloy foam sandwich panels. The optimal heat treatment time was determined through optimization of both the structural porosity of the foam and the tensile properties of the resultant AFS panel. The results of the tests indicated that the prepared AFS panel displayed a porosity ranging from 60 to 85% at a holding temperature of 948 K and holding time of 12 min or more. In the tensile tests, all fractures occurred within the foam structure, thus demonstrating the increased reliability of the AFS panels produced through FSW.

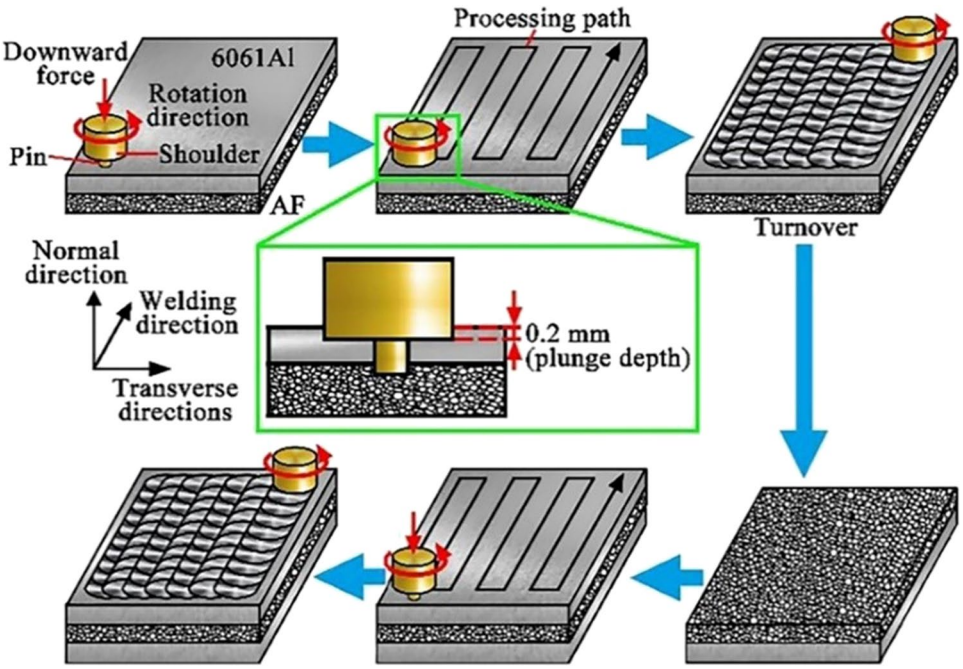

Fig. 15 The schematic of AFS preparation of 6061 Al by FSW [47]

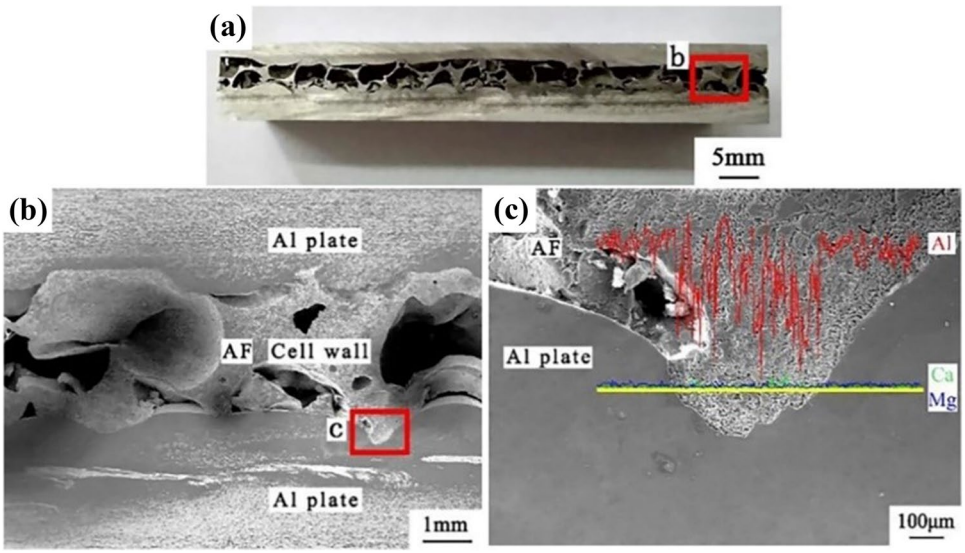

Fig. 16 The cross-sectional morphology of the AFS: (**a**) macroscopic morphology, (**b**) microstructure of the area labelled (**b**), and (**c**) microstructure and EDS results of the area labelled (**c**) [47]

In conclusion, the application of FSW to the preparation of foam metal offers numerous advantages over conventional fusion welding techniques. Not only does it enable the foaming of metals such as Al and Cu, but it also enables the establishment of secure connections between foam and solid panels. As a solid-state, low-temperature pressure welding method, the process of FSW eliminates welding defects related to melting and solidification, as well as any resultant joint area brittleness. Its features, including ease of mechanization and automation, high efficiency, minimal workpiece deformation, high dimensional accuracy, and absence of filler wire requirements, help in avoiding substantial densification of foam metal, thereby yielding improved tensile, bending, impact, and sound absorption properties. However, it must be noted that the reliance on the stirring head for frictional heat generation and pressure application, along with the inevitable movement and rotation of the stirring needle during the welding process, may cause some degree of damage to the foam structure. Additionally, the formation of a keyhole at the end of the weld, after the stirring head has departed, necessitates additional processes. Despite these limitations, the complete foam structure of the joints prepared through FSW proves suitable for functional and structural applications, given its ability to meet the demands of some functional parts and exhibit desirable mechanical properties.

3.2 Ultrasonic welding of foam metal/sheet metal

Ultrasonic welding is both pressure and solid-state welding. Unlike conventional welding processes, ultrasonic welding does not rely on the application of electrical currents or high-temperature heat sources. Instead, it utilizes the energy generated by the vibration of the welding head to create friction, deformation, and localized temperature rises between the workpieces under static pressure, thereby facilitating solid-phase connections between dissimilar metals. This welding process effectively eliminates the occurrences of spatter and oxidation associated with fusion welding, while avoiding the welding defects that stem from melting and solidification processes [58–60].

The application of ultrasonic welding is not limited to a specific metallurgical composition and offers a wide range of welding capabilities, including spot welding, seam welding, torsion welding, and other forms of welding for non-ferrous materials and thin wires such as Cu, Ag, Al, Ni, and others (Fig. 17). This welding method offers several advantages, including the absence of metallurgical restrictions, a broad welding range, suitability for precision welding, reduced dependence on surface cleanliness of the workpieces, and high welding efficiency. As a result, it has garnered widespread application in the fields of battery collection, precision electrical component preparation, aerospace, and automotive light-weighting initiatives [61–63].

The unique properties of ultrasonic welding have motivated several researchers to explore its use in the preparation of foam sandwich structures and FM/SM welded joints [30, 31, 42, 43]. Born et al. [42, 43] conducted a comprehensive examination of the ultrasonic torsional welding process for foam metal and sheet metal and investigated the feasibility and weldability of ultrasonic torsional, spot, and seam welding techniques for Al foam/sheet metal sandwich structures. Microscopic and mechanical property analysis indicated that ultrasonic torsional welding technology is capable of achieving an effective connection between foam metal and sheet metal without inducing significant deformation, with tensile shear strength reaching up to 25 MPa. The fatigue strength of the AFS was observed to be in the range of 18%, while the ultrasonic welding process did not significantly affect the holes in the Al foam and maintained the structural integrity of the foam metal to the greatest extent possible.

In recent years, Feng et al. [30, 31] sought to harness the capabilities of ultrasonic welding to achieve the welding of highly porous, open-cell foam metal to sheet metal, conducting extensive studies into the microstructure, mechanical properties, and connection mechanisms of the resulting joint. The Cu foam utilized in the study was fabricated through electrodeposition and possessed a porosity of up to 98% and an average pore size of 0.1 mm. The equipment and joint configuration utilized for the preparation of the highly porous open-cell FM/SM ultrasonic spot welding (USW) head is depicted in Fig. 18a. The ultrasonic welding head tip area measures 8 mm × 8 mm, with its pattern shape and tip tooth size shown in Fig. 18b and c, respectively. The joint is realized in the form of an Al-on-Cu lap joint.

In Fig. 19a–d, the evolution of the cross-sectional morphology of the ultrasonic weld between the open-cell Cu foam and the solid Al sheet is presented as a function of the welding energy. As depicted in Fig. 19a, at low-energy parameters, the interface is characterized by partially discrete micro-connections. However, with an increase in the welding energy, as shown in Fig. 19b, the rate of effective connection at the interface is substantially enhanced. The complex interplay of normal and shear stresses, resulting in swirl-like and mechanical embedding effects, serve to augment the joint strength, as evident in the welding interface [64, 65]. In Fig. 19c and d, it is observed that with a further escalation in the welding energy, a more pronounced thinning of the Cu foam occurs, leading to a decline in joint strength. Under the influence of normal and shear stresses, the Cu foam side of the joint experiences some degree of densification and thinning, but the majority of the three-dimensional Cu foam skeleton structure remains relatively intact. To quantify the surface morphology of the joint, three-dimensional super depth-of-field microscopy was utilized to measure the indentation depth at different welding energies, as demonstrated in Fig. 20. The indentation depth

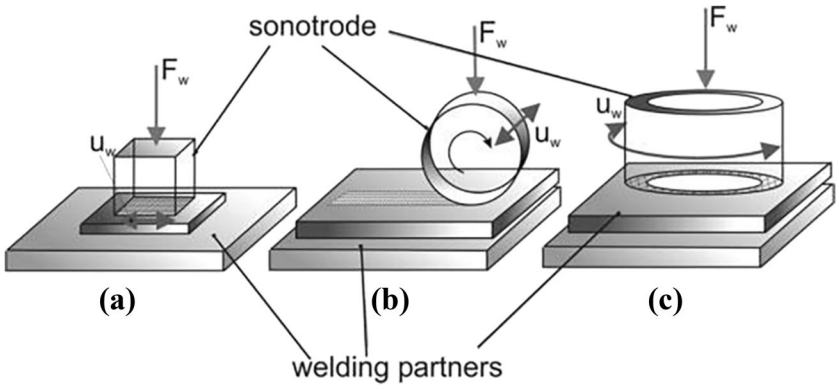

Fig. 17 The three different types of ultrasonic welding systems: (**a**) spot welding, (**b**) seam welding, and (**c**) torsion welding [43]

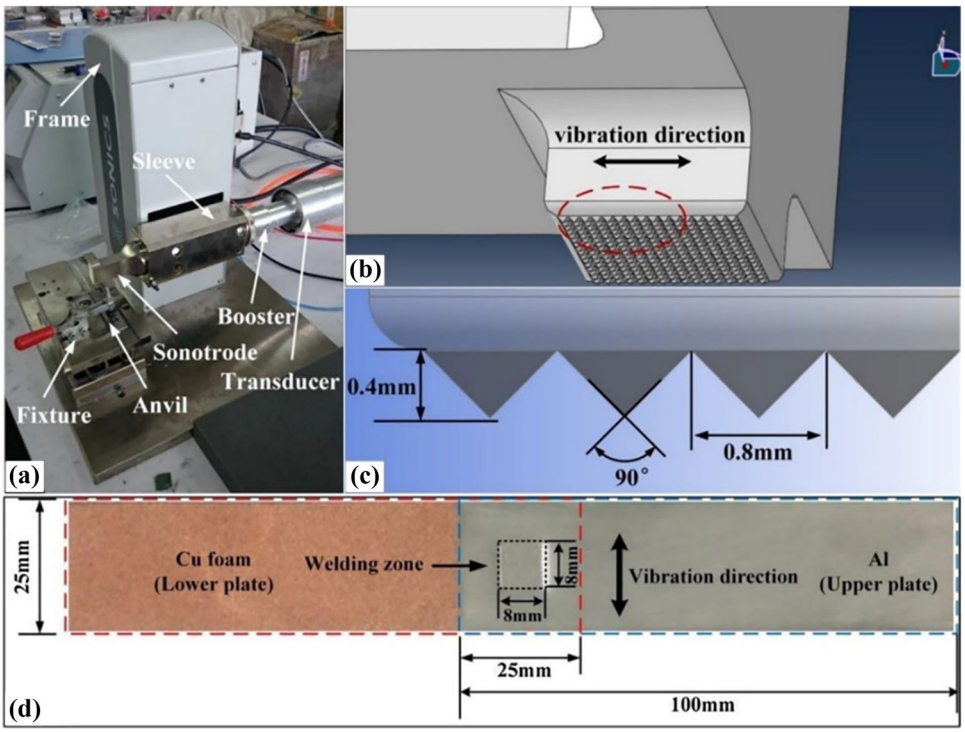

Fig. 18 The schematic diagram of USW system and lap joint: (**a**) main components of the USW system, (**b**) details of the horn, (**c**) size of the horn tooth tip, and (**d**) form of the lap joint of the welded specimen [30]

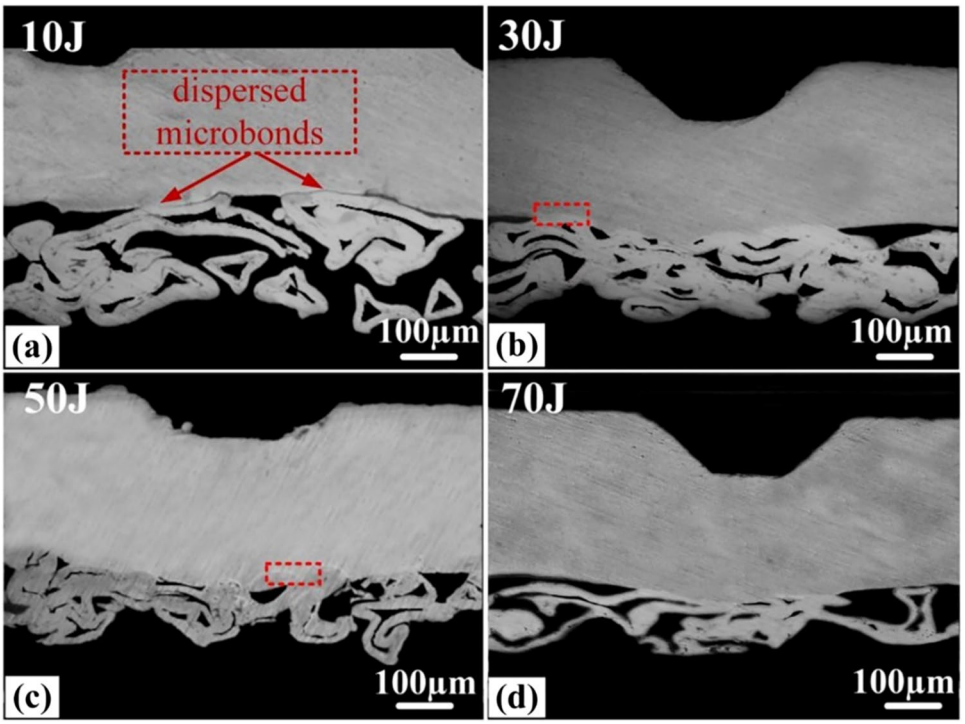

Fig. 19 The cross-sectional micromorphology of the FM/SM joints with different parameters: (**a**) 10 J, (**b**) 30 J, (**c**) 50 J, and (**d**) 70 J [30]

of the Cu foam side of the joint at different welding energies was found to be smaller than the average hole diameter of the Cu foam, which serves to affirm that USW can maintain the three-dimensional skeletal structure of the Cu foam during the welding process.

The results of the composition analysis of the open-cell Cu foam/Al sheet ultrasonic welding head interface reveal that the interface does not exhibit a discernible formation of intermetallic compounds. Rather, the diffusion of Al and Cu foam components is comparatively stable. The

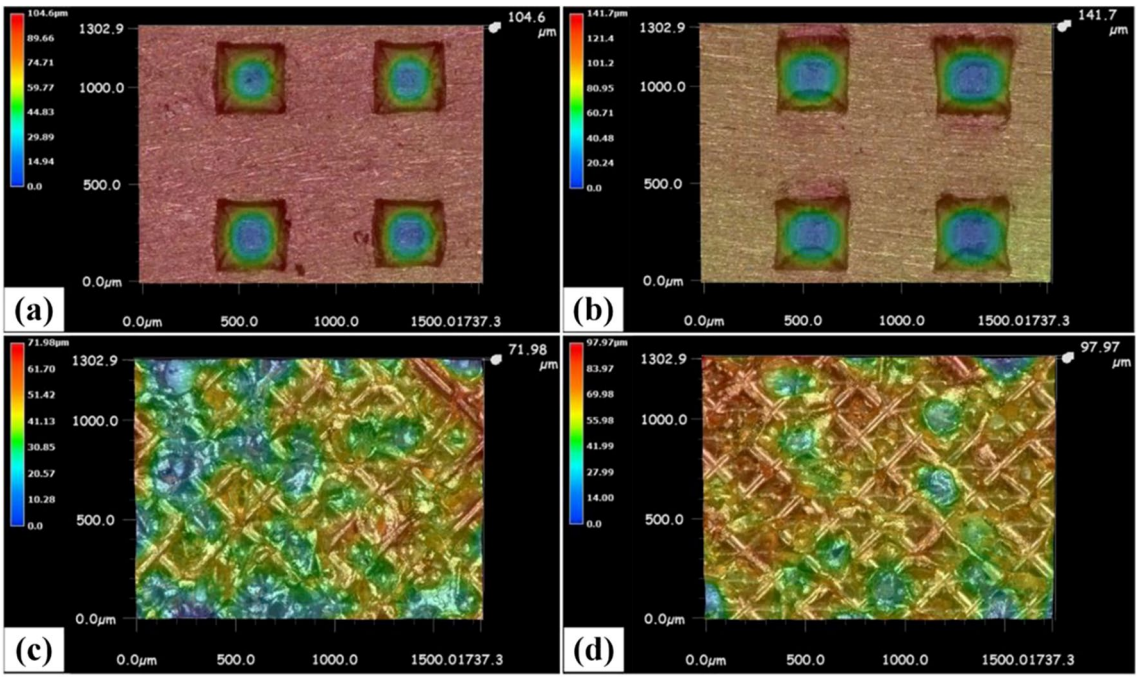

Fig. 20 The typical 3D morphology of the Al/Cu foam metal joints: (**a**) Al side of 30 J, (**b**) Al side of 70 J, (**c**) Cu foam side of 30 J, (**d**) Cu foam side of 70 J [30]

real-time infrared temperature field distribution analysis demonstrates that the highest temperature attained, 77.7°C at 70 J of welding energy, is significantly lower than the solid solution temperature of Al-Cu (548°C) [66]. This provides empirical validation that the connection mechanism of the Cu foam metal/Al sheet ultrasonic welding head is predominated by atomic diffusion and mechanical interlocking. The tensile strength of the joint is proportional to the effective density of the joint interface and the morphology of the foam side following welding. The maximum tensile load achieved for ultrasonic welding heads of Cu foam metal/Al sheet and Ni foam metal/Al sheet was 89.15% and 58.0%, respectively, of their respective foam base metal [30, 31]. Consequently, USW presents a viable means of establishing a secure connection between highly porous open-cell foam metal and Al sheets.

In conclusion, ultrasonic welding, as a method of solid-phase welding, is capable of forming a dependable connection between foam metal and sheet metal without inducing melting of the weld metal, thereby preserving the open-cell structure and inherent properties of the foam metal to a large extent. Nevertheless, its applications are limited to welding of sheets, wires, and other materials due to its power limitations. In terms of practical application, ultrasonic welding is geared towards welding of functional components, and the resulting joints possess also have a certain level of load-bearing capacity, making it suitable for thin foam metal that has functional requirements.

4 Brazing of foam metal

Brazing, as one of the earliest methods of joining materials utilized throughout human history, involves the connection of base materials through the application of a molten brazing material. During the brazing process, the brazing material transforms into a liquid state, while the base material remains in a solid form. The liquid brazing material permeates the gaps or surfaces of the base material through capillary action, filling and spreading, and then interacts with the base material, solidifying after a specific interval of time to form a solid joint [67–69]. As opposed to fusion welding, the brazing process does not require the melting of the base material, only the brazing material must be melted. Unlike pressure welding, brazing does not exert any pressure on the welded part. Typically, the heating temperature of brazing is much lower than the melting point of the base material, thereby having minimal impact on the physical and chemical properties of the base material. The uniform heating of the welded part leads to reduced stress and deformation, allowing for greater control of the dimensional accuracy and improved production efficiency.

The Ti-6Al-4V alloy, an α-β titanium alloy [70], is widely used within the aerospace industry due to its exceptional welding performance, corrosion resistance, and mechanical properties derived from its unique equilibrium phase. However, the conventional brazing process often results in reduced mechanical properties due to residual stresses

generated in the melt-flow-solidification process of the brazing material. The use of foam metal as a brazing material has emerged as an attractive alternative, as it offers advantageous properties such as energy absorption and buffering capabilities.

In a study by Jarvis et al. [39], the application of Ti-Cu-Ni alloy as a brazing material was explored for joining nickel foam with Ti-6Al-4V alloy. The macroscopic examination of the joint revealed a degree of porosity within the brazing layer, which may lead to crack formation under load as depicted in Fig. 21a. The presence of pores can have a significant impact on the joint's mechanical properties. The micromorphology, as illustrated in Fig. 21b, showed that the solder penetrated deep into the skeletal structure of the nickel foam and was drawn into the foam's pore structure via capillary action. This close bonding of the solder to the nickel foam resulted in a strong interface that contributed to the overall strength of the joint. The shear test results indicated that the joint possessed a yield stress of 1.27 MPa and an ultimate shear strength of 1.44 MPa, demonstrating good shear strength and ductility.

Ceramics, owing to their high melting point and consistent chemical properties, are widely acknowledged as a promising material for heat resistance across various industries, including aerospace, biomaterials, and electronics [71, 72]. Despite their attractive attributes, the brittleness of ceramics has been identified as a hindrance to its development, thus driving the trend of combining ceramics with metals in order to yield a novel composite material that embodies the superior qualities of both. To achieve this goal, various researchers have utilized metal powder, foil, or foam metal in the development of composite welding processes aimed at reducing residual stresses in the joint [73–77].

Wang et al. [78] sought to investigate the influence of AgCu/Cu foam composite brazing material on the performance of brazed joints between ZrB_2-SiC ceramics and Inconel 600 alloy. Figure 22a and b display the brazed joint assembly and shear strength test setup respectively, using a size of 4mm for both the Cu foam and AgCu brazing materials. The results indicate that the ZrB_2-SiC ceramics and Inconel 600 alloy brazed joints obtained through the application of AgCu and AgCu/Cu foam as composite brazing materials, held at 1173 K for 15 min, possess desirable joint properties, as demonstrated in Fig. 23. The fracture morphology of the joints is depicted in Fig. 23c–f, and it was observed that the presence of Cu (s, s) phase in the joints that employed AgCu/Cu foam as composite brazing material effectively reduced the residual stresses and improved the shear strength by 43 MPa compared to those that utilized AgCu brazing material solely. Similarly, Sun et al. [79] showed that the maximum residual stress in Al_2O_3/1Cr18Ni9Ti stainless steel joints brazed using AgCuTi-Ni as brazing material was significantly reduced from 449.9 to 74.7 MPa, with the addition of a Cu foam interlayer resulting in a 95% improvement in the shear strength compared to those without the interlayer.

Li et al. [80] identified, through examination of the results obtained from brazing trials on silicon nitride ceramics and

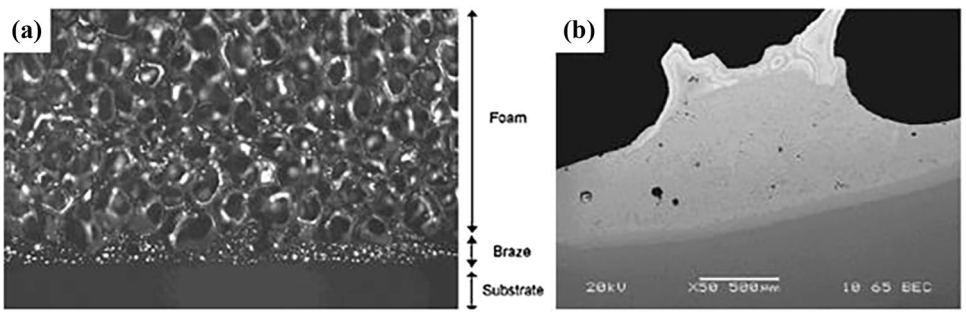

Fig. 21 The cross-sectional morphology of brazed joint of nickel foam: (**a**) low magnification microscope image of the bonded area, (**b**) SEM image of a localized weld joint [39]

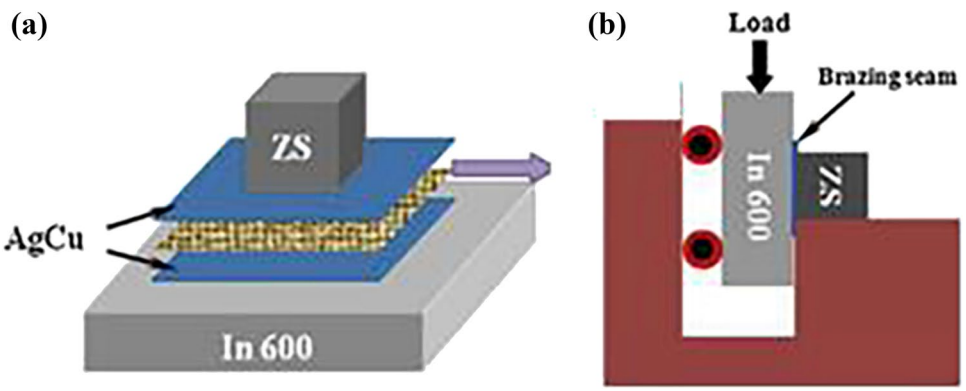

Fig. 22 The sketch of (**a**) lap brazing with the Cu foam as the interlayer and (**b**) tension-shear test of the joints assembly [78]

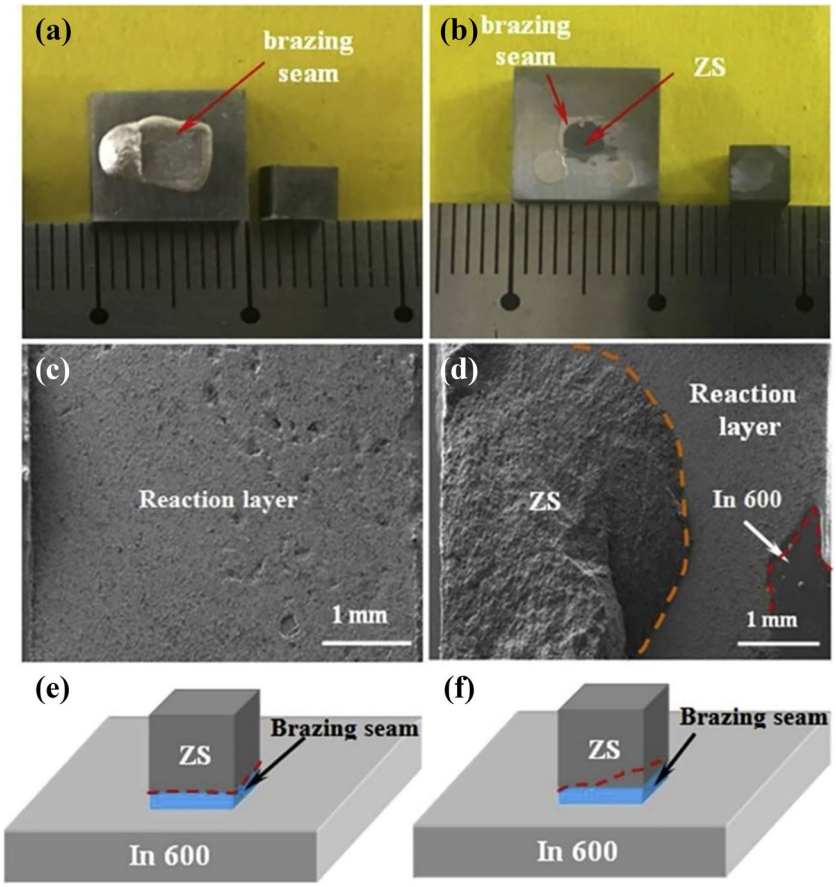

Fig. 23 The characterization of fracture surface in lap brazing without (**a**, **c**, and **e**) and with (**b**, **d**, and **f**) the Cu foam as interlayer [78]

$(TiB+Y_2O_3)$/Ti matrix composites, that when the brazing temperature underwent a marked increase, an elemental diffusion was triggered, leading to the formation of Ag(s, s) and Cu(s, s) phases within the joints. Upon reaching a temperature of 820°C, eutectic distribution was observed to be uniformly present throughout the joints, thus enhancing the joint properties, as depicted in Fig. 24. However, as the brazing temperature continued to rise to 840°C and 860°C, the mechanical properties of the joints diminished, owing to the collapse of the Cu foam and the proliferation of a substantial number of intermetallic compounds.

In essence, the brazing technique is a highly favored solution for applications necessitating stringent precision requirements, intricate configurations, limited accessibility to joint areas, and welding of dissimilar materials. Given its impressive ductile and energy-absorbing attributes, foam metal acts as a stress reducer in brazing, serving both as a welding material and an interlayer. However, the brazed joint's heat tolerance is limited, and elevating brazing temperature to excessive levels can result in the degradation of the foam's structure, leading to a decreased mechanical performance of the brazed joint. Unprocessed brazed joints, further, are often restricted in terms of strength, exacerbated by the frequent use of lap joints, thereby increasing the usage of base and brazing materials, as well as adding weight to the structure. In terms of application, foam metal should be viewed as an aid in the brazing process, primarily reflecting the functionality of the foam metal, instead of solely relying on brazing for welding foam metal.

5 Conclusion and scope for future research

The present study provides a comprehensive overview of recent advances and developments in the field of foam metal welding, incorporating insights gleaned from contemporary research and scholarly inquiries into fusion welding, pressure welding, and brazing techniques. To establish the link between the application and the welding technology of foam metal, the paper first offers a succinct overview of the distinctive features, performance characteristics, and potential applications of foam metal, as well as the challenges inherent to the welding process.

With respect to fusion welding, it has been demonstrated that the resulting foam-welded joints exhibit remarkable load-bearing capacity. However, as with traditional solid-sheet welding, the fusion welding of foam metal is also susceptible to a range of welding defects, including porosity, burn-through, and incomplete penetrations. The unique

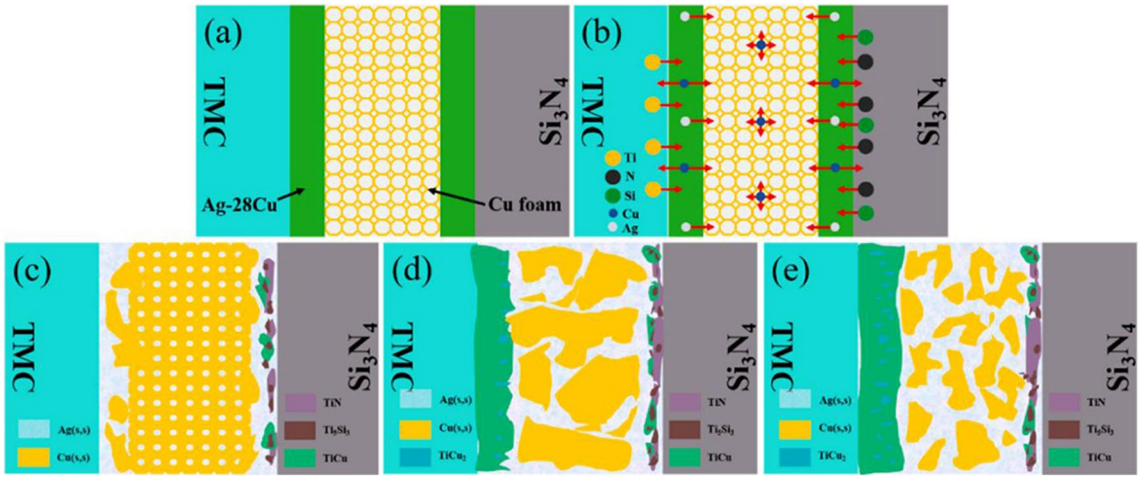

Fig. 24 The schematic diagram of the formation mechanism of the TMC/Si N brazed joint: (**a**) the cross-section of the samples, (**b**) the diffusion of elements, (**c**) the formation of a small amount of TiCu phases, (**d**) the formation of a small amount of $TiCu_2$ phases, (**e**) the well connection between the TMCs and the Si_3N_4

structure of foam metal further exacerbates these difficulties, as slumping and densification of the pores can occur during the welding process. While some degree of slumping and densification can be beneficial in the creation of a foam weld, as it allows the molten metal to fill in small contact areas that would otherwise be difficult to join, excessive slumping and densification can lead to high stress concentrations in the joint and a subsequent reduction in joint strength.

The pressure welding technique enables the acquisition of both functional and structural welded joints in foam metal, with the selection of the most appropriate pressure welding method contingent on the requirements and focus of the particular application. FSW can not only facilitate the foaming of Al foam, but also provide reliable connections in Al foam–solid Al sandwich structures. The resulting joints exhibit robust load-bearing capacity and boast advantageous impact and sound absorption characteristics, owing to the minimization of foam pore collapse. As a solid-phase welding method, ultrasonic welding can create a secure connection without undergoing metal melting; the welded joint retains the maximum extent of the foam metal's structural and functional characteristics, and simultaneously possesses a noteworthy load-bearing capacity, making it appropriate for the welding of sheets and wire materials.

Brazing, as a more specific technique in the joining of foam metal, is primarily aimed at enhancing the functionality of the foam metal, rather than welding its joints. The foam metal serves as a supportive medium in the brazing process, sometimes as a base material and other times as an interlayer, both with the objective of assisting the release of residual stresses generated during the brazing process. Inadequate joints can result from low brazing temperatures and pressures, thus impeding the functionality of the foam, whereas high temperatures can lead to collapse and densification of the foam pores, resulting in loss of functionality.

The mechanical properties of foam joints are crucial in the context of the material's application and the choice of welding method. The mechanical properties of welded structural joints of foam metal are typically evaluated using tensile testing, which offers isolated results and lacks a comprehensive analysis and understanding of fracture. In order to make a comprehensive selection of the welding method and properly specify the welding process, a more comprehensive means of evaluating the mechanical properties is necessary, entailing the establishment of a constitutive model of the material joint, the exploration of the mechanical properties of the joint from multiple perspectives, and the observation and analysis of fracture morphology.

The functional retention of a foam joint is an integral criterion in assessing the efficacy of the welding process. The application of high-porosity open-cell foam metal as functional components in industrial production is widely acknowledged due to their unique characteristics such as heat exchange, electrical conductivity, and electromagnetic shielding properties. The foam metal's three-dimensional internal skeleton structure contributes to its unique properties; however, welding can potentially damage the pore structure and result in a diminished or even lost functional joint. Currently, there is a lack of standard methods for characterizing the functionality of foam joints, highlighting the need for more comprehensive methods of testing functionality and increased research into functionality in various application scenarios.

The microscopic morphology and organization at the weld joint play a crucial role in the development of the welding process. Any adjustments made to the welding process can directly impact welding defects and results, leading to changes

in the mechanical properties of the joint. Currently, only metallographic and SEM are used to observe the morphological and microstructural characteristics of foam metal joints, lacking an analysis of grain size and texture. Increased examination of the grain scale at the foam metal's joint weld will provide a better understanding of the effect of different welding methods on the material's structure, thereby providing a solid theoretical foundation for evaluating the joint's mechanical properties and other performance indicators.

The introduction of advanced non-destructive monitoring techniques such as industrial CT and 3D X-ray imaging has the potential to address these difficulties in adjusting the welding process due to the randomness of the foam structure and contribute to the advancement of the foam simulation field. Currently, research in foam metal welding simulation is in its nascent stages, and the use of modeling and algorithms can help to comprehend the heat transfer, plastic deformation, and thermodynamic calculations of the welding process, which is essential for optimizing the joint's performance and regulating the composition of the weld.

With regard to optimizing the functionality of foam metal–welded joints, future research endeavors could focus on achieving greater precision in controlling the joint inputs in order to attain better performing joints. In particular, fusion welding techniques could be refined through precise control of the heat source input, in an effort to maintain the integrity of the foam metal's three-dimensional skeleton structure while ensuring adequate load-bearing capacity of the joint. This is particularly challenging given the low actual contact area between the foam metal's skeleton structure and the weld contact surface. To address this issue, it is crucial to identify and employ an appropriate interlayer material to enhance the reliability and effectiveness of the joint.

It is essential to consider both the structural and functional aspects of the foam metal when assessing its overall performance, especially in regard to single structural components. In these cases, it is desirable to retain as much of the foam metal's functionality as possible while preserving its load-bearing capabilities. To achieve this balance, it is necessary to continually make trade-offs between the structural and functional properties of the joint, depending on the specific application scenario of the foam metal, and to adjust the welding process accordingly in order to optimize the joint's overall performance.

Author contributions The inception and design of this study were a collective effort among all authors. The initial conception of the thesis was carried out by Mengnan Feng and Peng Wang, who further reviewed and revised the first draft. The primary draft of the manuscript was meticulously crafted by Liang Ren. The literature collection was carried out by Ziyao Wang, Dequan Meng, and Shuo Wang, who further provided insightful comments on earlier versions of the manuscript. Finally, all authors meticulously reviewed and approved the final manuscript prior to its submission.

Funding This work was supported by the National Natural Science Foundation of China (Grant No. 51905358) and Natural Science Foundation of Hebei Province (Grant Nos. E2020210077 and E2020210095).

Data availability Not applicable.

Code availability Not applicable.

Declarations

Ethics approval Not applicable.

Consent to participate Not applicable.

Consent for publication Not applicable.

Conflict of interest The authors declare no competing interests.

References

1. Banhart J, Ashby M, Fleck N (1999) Metal foams and porous metal structures. In: Metal Foams and Porous Metal Structures, vol 56, pp 14–16
2. Baumgärtner F, Duarte I, Banhart J (2000) Industrialization of powder compact toaming process. Adv Eng Mater 2(4):168–174. https://doi.org/10.1002/(SICI)1527-2648(200004)2:4<168::AID-ADEM168>3.0.CO;2-O
3. Fusheng H, Zhengang Z (1999) The mechanical behavior of foamed aluminum. J Mater Sci 34(2):291–299. https://doi.org/10.1023/A:1004401521842
4. Zardiackas LD, Parsell DE, Dillon LD, Mitchell DW, Nunnery LA, Poggie R (2001) Structure metallurgy and mechanical properties of a porous tantalum foam. J Biomed Mater Res 58(2):180–187. https://doi.org/10.1002/1097-4636(2001)58:2<180::AID-JBM1005>3.0.CO;2-5
5. Imwinkelried T (2007) Mechanical properties of open-pore titanium foam. J Biomed Mater Res A 81(4):964–970. https://doi.org/10.1002/jbm.a.31118
6. Dinesh BVS, Bhattacharya A (2020) Comparison of energy absorption characteristics of PCM-metal foam systems with different pore size distributions. J Energy Storage 28:101190. https://doi.org/10.1016/j.est.2019.101190
7. Guo J, Liu Z, Du Z, Yu J, Yang X, Yan J (2021) Effect of fin-metal foam structure on thermal energy storage: an experimental study. Renew Energy 172:57–70. https://doi.org/10.1016/j.renene.2021.03.018
8. Sevilla P, Aparicio C, Planell JA, Gil FJ (2007) Comparison of the mechanical properties between tantalum and nickel-titanium foams implant materials for bone ingrowth applications. J Alloys Compd 439(1-2):67–73. https://doi.org/10.1016/j.jallcom.2006.08.069
9. Sun G, Wang Z, Yu H, Gong Z, Li Q (2019) Experimental and numerical investigation into the crashworthiness of metal-foam-composite hybrid structures. Compos Struct 209:535–547. https://doi.org/10.1016/j.compstruct.2018.10.051
10. Ji K, Zhao H, Huang Z, Dai Z (2014) Performance of open-cell foam of Cu-Ni alloy integrated with graphene as a shield against electromagnetic interference. Mater Lett 122:244–247. https://doi.org/10.1016/j.matlet.2014.02.025
11. Queheillalt DT, Katsumura Y, Wadley HNG (2004) Synthesis of stochastic open cell Ni-based foams. Scr Mater 50(3):313–317. https://doi.org/10.1016/j.scriptamat.2003.10.016
12. Aramesh M, Shabani B (2022) Metal foam-phase change material composites for thermal energy storage: a review of

performance parameters. Renewable Sustainable Energy Rev 155:111919. https://doi.org/10.1016/j.rser.2021.111919
13. Li H, Chen S, He M, Jin J, Zhu K, Peng F, Gao F (2022) Self-supported V-doped NiO electrocatalyst achieving a high ammonia yield of 30.55 μg h^{-1} cm^{-2} under ambient conditions. New J Chem. https://doi.org/10.1039/d2nj02867k
14. Changdar A, Chakraborty SS (2021) Laser processing of metal foam - a review. J Manuf Process 61:208–225. https://doi.org/10.1016/j.jmapro.2020.10.012
15. Yu CF, Lin LY (2016) Effect of the bimetal ratio on the growth of nickel cobalt sulfide on the Ni foam for the battery-like electrode. J Colloid Interface Sci 482:1–7. https://doi.org/10.1016/j.jcis.2016.07.059
16. Bidault F, Brett DJL, Middleton PH, Abson N, Brandon NP (2009) A new application for nickel foam in alkaline fuel cells. Int J Hydrog Energy 34(16):6799–6808. https://doi.org/10.1016/j.ijhydene.2009.06.035
17. Zhou ZQ, Lin GW, Zhang JL, Ge JS, Shen JR (1999) Degradation behavior of foamed nickel positive electrodes of Ni-MH batteries. J Alloys Compd 293-295:795–798. https://doi.org/10.1016/s0925-8388(99)00465-x
18. Longerich S, Piontek D, Ohse P, Harms A, Dilthey U, Angel S, Bleck W (2007) Joining strategies for open porous metallic foams on iron and nickel base materials. Adv Eng Mater 9(8):670–678. https://doi.org/10.1002/adem.200700114
19. Banhart J (2001) Manufacture, characterisation and application of cellular metals and metal foams. Prog Mater Sci 46(6):559–632. https://doi.org/10.12691/ajme-6-3-5
20. Wang L, Xie Y, Wei C, Lu X, Li X, Song Y (2015) Hierarchical NiO superstructures/foam Ni electrode derived from Ni metal-organic framework flakes on foam Ni for glucose sensing. Electrochim Acta 174:846–852. https://doi.org/10.1016/j.electacta.2015.06.086
21. Jiang T, Zhang S, Qiu X, Zhu W, Chen L (2007) Preparation and characterization of silicon-based three-dimensional cellular anode for lithium ion battery. Electrochem Commun 9(5):930–934. https://doi.org/10.1016/j.elecom.2006.11.031
22. Fan X, Zhuang Q, Jiang H, Huang L, Dong Q, Sun S (2007) Three-dimensional porous Cu6Sn5 alloy anodes for lithium-ion batteries. Acta Phys-Chimica Sin 23(7):973–977. https://doi.org/10.1016/s1872-1508(07)60051-5
23. Chen C, Wu J, Li H (2021) Optimization design of cylindrical rivet in flat bottom riveting. Thin-Walled Struct 168:108292. https://doi.org/10.1016/j.tws.2021.108292
24. Li H, Yi R, Chen C (2022) Microstructure and mechanical performance of dissimilar material joints of 2024Al and SiO2 glass by ultrasonic assisted soldering with Cu interlayer. J Mater Res Technol 18:3227–3239. https://doi.org/10.1016/j.jmrt.2022.03.155
25. Peng H, Chen C, Ren X, Ran X, Gao X (2021) Research on the material flow and joining performance of two-strokes flattening clinched joint. Thin-Walled Struct 169:108289. https://doi.org/10.1016/j.tws.2021.108289
26. Qin D-L, Chen C (2022) Failure behavior and mechanical properties of novel dieless clinched joints with different sheet thickness ratios. J Cent South Univ 29(9):3077–3087. https://doi.org/10.1007/s11771-022-5120-8
27. Ran X, Chen C, Zhang H, Ouyang Y (2021) Investigation of the clinching process with rectangle punch. Thin-Walled Struct 166:108034. https://doi.org/10.1016/j.tws.2021.108034
28. Shi C, Li H, Chen C, Ouyang Y, Qin D (2022) Experimental investigation of the flat clinch-rivet process. Thin-Walled Struct 171:108612. https://doi.org/10.1016/j.tws.2021.108612
29. Zhang X, Chen C (2022) Experimental investigation of joining aluminum alloy sheets by stepped mechanical clinching. J Mater Res Technol 19:566–577. https://doi.org/10.1016/j.jmrt.2022.05.046
30. Feng M-N, Xie Y, Zhao C-F, Luo Z (2018) Microstructure and mechanical performance of ultrasonic spot welded open-cell Cu foam/Al joint. J Manuf Process 33:86–95. https://doi.org/10.1016/j.jmapro.2018.04.022
31. Xie Y, Feng M, Cai Y, Luo Z (2017) Ultrasonic spot welding of nickel foam sheet and aluminum solid sheet. Adv Eng Mater 19(8). https://doi.org/10.1002/adem.201700094
32. Crupi V, Montanini R (2007) Aluminium foam sandwiches collapse modes under static and dynamic three-point bending. Int J Impact Eng 34(3):509–521. https://doi.org/10.1016/j.ijimpeng.2005.10.001
33. Biffi CA, Colombo D, Tuissi A (2014) Laser beam welding of CuZn open-cell foams. Opt Lasers Eng 62:112–118. https://doi.org/10.1016/j.optlaseng.2014.05.005
34. Biffi CA, Casati R, Previtali B, Tuissi A (2016) Microstructure and mechanical properties of laser welded beads realized for joining CuZn open cellular foams. Mater Lett 181:132–135. https://doi.org/10.1016/j.matlet.2016.05.161
35. Biffi CA, Previtali B, Tuissi A (2017) Microstructure and calorimetric behavior of laser welded open cell foams in CuZnAl shape memory alloy. Funct Mater Lett 09(06). https://doi.org/10.1142/s1793604716420078
36. Oliveira JP, Panton B, Zeng Z, Omori T, Zhou Y, Miranda RM, Braz Fernandes FM (2016) Laser welded superelastic Cu-Al-Mn shape memory alloy wires. Mater Des 90:122–128. https://doi.org/10.1016/j.matdes.2015.10.125
37. Haferkamp H, Bunte J, Herzog D, Ostendorf A (2013) Laser based welding of cellular aluminium. Sci Technol Weld Join 9(1):65–71. https://doi.org/10.1179/136217104225017170
38. Tan JC, Westgate SA, Clyne TW (2013) Resistance welding of thin stainless steel sandwich sheets with fibrous metallic cores: experimental and numerical studies. Sci Technol Weld Join 12(6):490–504. https://doi.org/10.1179/174329307x213666
39. Jarvis T, Voice W, Goodall R (2011) The bonding of nickel foam to Ti-6Al-4V using Ti-Cu-Ni braze alloy. Mater Sci Eng: A 528(6):2592–2601. https://doi.org/10.1016/j.msea.2010.11.077
40. Kitazono K, Kitajima A, Sato E, Matsushita J, Kuribayashi K (2002) Solid-state diffusion bonding of closed-cell aluminum foams. Mater Sci Eng: A 327(2):128–132. https://doi.org/10.1016/S0921-5093(01)01766-X
41. Liu C, Zhu Z, Han F, Banhart J (1998) Internal friction of foamed aluminium in the range of acoustic frequencies. J Mater Sci 33(7):1769–1775
42. Born C, Kuckert H, Wagner G, Eifler D (2003) Ultrasonic torsion welding of sheet metals to cellular metallic materials. Adv Eng Mater 5(11):779–786. https://doi.org/10.1002/adem.200310102
43. Born C, Wagner G, Eifler D (2006) Ultrasonically welded aluminium foams/sheet metal - joints. Adv Eng Mater 8(9):816–820. https://doi.org/10.1002/adem.200600083
44. Ni ZL, Yang JJ, Hao YX, Chen LF, Li S, Wang XX, Ye FX (2020) Ultrasonic spot welding of aluminum to copper: a review. Int J Adv Manuf Technol 107(1-2):585–606. https://doi.org/10.1007/s00170-020-04997-5
45. Nowacki J, Moraniec K (2015) Welding of metallic AlSi foams and AlSi-SiC composite foams. Arch Civ Mech Eng 15(4):940–950. https://doi.org/10.1016/j.acme.2015.02.007
46. Böllinghaus T, Von Hagen H, Bleck W, Werden Aluminium H (2000) Laserstrahlschweißen von schäumbarem Aluminiumhalbzeug. UTF. Science 11:23–26
47. Peng P, Wang K, Wang W, Huang L, Qiao K, Che Q, Xi X, Zhang B, Cai J (2019) High-performance aluminium foam sandwich prepared through friction stir welding. Mater Lett 236:295–298. https://doi.org/10.1016/j.matlet.2018.10.125
48. Hangai Y, Kamada H, Utsunomiya T, Kitahara S, Kuwazuru O, Yoshikawa N (2014) Aluminum alloy foam core sandwich panels fabricated from die casting aluminum alloy by friction stir welding route. J Mater Process Technol 214(9):1928–1934. https://doi.org/10.1016/j.jmatprotec.2014.04.010

49. Shih J-S, Tzeng Y-F, Yang J-B (2011) Principal component analysis for multiple quality characteristics optimization of metal inert gas welding aluminum foam plate. Mater Des 32(3):1253–1261. https://doi.org/10.1016/j.matdes.2010.10.001
50. Zuo X, Zhang W, Chen Y, Oliveira JP, Zeng Z, Li Y, Luo Z, Ao S (2022) Wire-based directed energy deposition of NiTiTa shape memory alloys: microstructure, phase transformation, electrochemistry, X-ray visibility and mechanical properties. Addit Manuf 59. https://doi.org/10.1016/j.addma.2022.103115
51. Hangai Y, Utsunomiya T (2008) Fabrication of porous aluminum by friction stir processing. Metall Mater Trans A 40(2):275–277. https://doi.org/10.1007/s11661-008-9733-9
52. Ashby MF, Evans T, Fleck NA, Hutchinson J, Wadley H, Gibson L (2000) Metal foams: a design guide. Elsevier 16(5):13-16.
53. Banhart J (2013) Light-metal foams-history of innovation and technological challenges. Adv Eng Mater 15(3):82–111. https://doi.org/10.1002/adem.201200217
54. Sathiskumar R, Murugan N, Dinaharan I, Vijay S (2013) Role of friction stir processing parameters on microstructure and microhardness of boron carbide particulate reinforced copper surface composites. Sadhana 38(6):1433–1450. https://doi.org/10.1007/s12046-013-0184-7
55. Nisa SU, Pandey S, Pandey PM (2020) Formation and characterization of 6063 aluminum metal foam using friction stir processing route. Mater Today: Proc 26:3223–3227. https://doi.org/10.1016/j.matpr.2020.02.903
56. Hangai Y, Takada K, Fujii H, Aoki Y, Utsunomiya T (2019) Foaming behavior of blowing- and stabilization-agent-free aluminum foam precursor during spot friction stir welding. J Mater Process Technol 265:185–190. https://doi.org/10.1016/j.jmatprotec.2018.10.013
57. Sharma VM, Pal SK, Racherla V (2021) Fabrication of copper foam using friction processing. Manuf Lett 29:61–64. https://doi.org/10.1016/j.mfglet.2021.06.004
58. Sanga B, Wattal R, Nagesh D (2018) Mechanism of joint formation and characteristics of interface in ultrasonic welding: literature review. Period Eng Nat Sci 6(1):107–119. https://doi.org/10.21533/pen.v6i1.158
59. Tao W, Su X, Wang H, Zhang Z, Li H, Chen J (2019) Influence mechanism of welding time and energy director to the thermoplastic composite joints by ultrasonic welding. J Manuf Process 37:196–202. https://doi.org/10.1016/j.jmapro.2018.11.002
60. Daniels H (1965) Ultrasonic welding. Ultrasonics 3(4):190–196. https://doi.org/10.1016/0041-624X(65)90169-1
61. Zhang G-P, Li J-C, Liu Z-X, Wang P-C (2020) Application of ultrasonic welding to repair adhesively bonded short carbon fiber reinforced Nylon 6 composites. Int J Adhes Adhes 100:102603. https://doi.org/10.1016/j.ijadhadh.2020.102603
62. Kumar S, Wu C, Padhy G, Ding W (2017) Application of ultrasonic vibrations in welding and metal processing: a status review. J Manuf Process 26:295–322. https://doi.org/10.1016/j.jmapro.2017.02.027
63. Matheny M, Graff K (2015) Ultrasonic welding of metals in power ultrasonics, vol 259-293. Elsevier. https://doi.org/10.1016/B978-1-78242-028-6.00011-9
64. Yang Y, Ram GJ, Stucker B (2009) Bond formation and fiber embedment during ultrasonic consolidation. J Mater Process Technol 209(10):4915–4924. https://doi.org/10.1016/j.jmatprotec.2009.01.014
65. Zhao Y, Li D, Zhang Y (2013) Effect of welding energy on interface zone of Al-Cu ultrasonic welded joint. Sci Technol Weld Join 18(4):354–360. https://doi.org/10.1179/1362171813Y.0000000114
66. Yang J, Cao B, He X, Luo H (2014) Microstructure evolution and mechanical properties of Cu-Al joints by ultrasonic welding. Sci Technol Weld Join 19(6):500–504. https://doi.org/10.1179/1362171814Y.0000000218
67. Klocke F, Castell-Codesal A, Donst D (2005) Process characteristics of laser brazing aluminium alloys. Adv Mat Res 36:135–142. https://doi.org/10.4028/www.scientific.net/AMR.6-8.135
68. Zhou L, Zhu S, Zheng W, Li T, Wu L, Zhang Z, Lei Z (2020) Constant current induction brazing process optimization of AgCdO15-Cu electrical contact. J Manuf Process 51:122–129. https://doi.org/10.1016/j.jmapro.2020.01.022
69. Takemoto T, Okamoto I (1988) Intermetallic compounds formed during brazing of titanium with aluminium filler metals. J Mater Sci 23(4):1301–1308. https://doi.org/10.2464/jilm.36.627
70. Li Y, Chen C, Yi R, Ouyang Y (2020) Review: Special brazing and soldering. J Manuf Process 60:608–635. https://doi.org/10.1016/j.jmapro.2020.10.049
71. He R, Hu P, Zhang X, Han W, Wei C, Hou Y (2013) Preparation of high solid loading, low viscosity ZrB2-SiC aqueous suspensions using PEI as dispersant. Ceram Int 39(3):2267–2274. https://doi.org/10.1016/j.ceramint.2012.08.073
72. Hu P, Wang Z (2010) Flexural strength and fracture behavior of ZrB2-SiC ultra-high temperature ceramic composites at 1800° C. J Eur Ceram Soc 30(4):1021–1026. https://doi.org/10.1016/j.jeurceramsoc.2009.09.029
73. Cui B, Huang JH, Xiong JH, Zhang H (2013) Reaction-composite brazing of carbon fiber reinforced SiC composite and TC4 alloy using Ag-Cu-Ti-(Ti+ C) mixed powder. Mater Sci Eng: A 562:203–210. https://doi.org/10.1016/j.msea.2012.11.031
74. Feng J, Liu D, Zhang L, Lin X, He P (2010) Effects of processing parameters on microstructure and mechanical behavior of SiO2/Ti-6Al-4V joint brazed with AgCu/Ni interlayer. Mater Sci Eng: A 527(6):1522–1528. https://doi.org/10.1016/j.msea.2009.10.050
75. Kim T, Park SW (2000) Effects of interface and residual stress on mechanical properties of ceramic/metal system. Key Eng Mater 183:1279–1284. https://doi.org/10.4028/www.scientific.net/KEM.183-187.1279
76. Wang X, Cheng L, Fan S, Zhang L (2012) Microstructure and mechanical properties of the GH783/2.5 DC/SiC joints brazed with Cu-Ti+ Mo composite filler. Mater Des 1980-2015 36:499–504. https://doi.org/10.1016/j.matdes.2011.11.058
77. Zaharinie T, Moshwan R, Yusof F, Hamdi M, Ariga T (2014) Vacuum brazing of sapphire with Inconel 600 using Cu/Ni porous composite interlayer for gas pressure sensor application. Mater Des 1980-2015(54):375–381. https://doi.org/10.1016/j.matdes.2013.08.046
78. Wang G, Cai Y, Wang W, Gui K, Zhu D, Tan C, Cao W (2019) Brazing ZrB2-SiC ceramics to Inconel 600 alloy without and with Cu foam. J Manuf Process 41:29–35. https://doi.org/10.1016/j.jmapro.2019.03.023
79. Sun R, Zhu Y, Guo W, Peng P, Li L, Zhang Y, Fu J, Li F, Zhang L (2018) Microstructural evolution and thermal stress relaxation of Al2O3/Cr18Ni9Ti brazed joints with nickel foam. Vacuum 148:18–26. https://doi.org/10.1016/j.vacuum.2017.10.030
80. Li M, Shi K, Zhu D, Dong D, Liu L, Wang X (2021) Microstructure and mechanical properties of Si3N4 ceramic and (TiB + Y2O3)/Ti matrix composite joints brazed with AgCu/Cu foam/AgCu multilayered filler. J Manuf Process 66:220–227. https://doi.org/10.1016/j.jmapro.2021.04.025